JLAB-PHY-09-993

Theory Support for the Excited Baryon Program at the JLab 12 GeV Upgrade*

I. Aznauryan,[1,2] V. Braun,[3] V. Burkert,[1] S. Capstick,[4] R. Edwards,[1]
I.C.Cloet,[5] M. Giannini,[6] T.-S. H. Lee,[1,7] H.-W. Lin,[1] V. Mokeev,[1,8]
C.D. Roberts,[7] E. Santopinto,[9] P. Stoler,[10] Q. Zhao,[11] and B.S. Zou[11]

[1] *Thomas Jefferson National Accelerator Facility, Newport News, VA 23606, USA*

[2] *Yerevan Physics Institute, 375036 Yerevan, Armenia*

[3] *Institute for Theoretical Physics, University of Regensburg, 93040,Regengurg, Germany*

[4] *Department of Physics, Florida State University, USA*

[5] *Department of Physics, University of Washington, Seattle, WA 98195, USA*

[6] *University of Genova and National Institute of Nuclear Physics. Genova, Via Dodecaneso, 33, Italy*

[7] *Physics Division, Argonne National Laboratory, Argonne, IL 60439, USA*

[8] *Skobeltsyn Nuclear Physics Institute at Moscow State University, Moscow 119899, Leninskie gory, OEPVAYa, Russia*

[9] *National Institute of Nuclear Physics. Genova, Via Dodecaneso, 33, Italy*

[10] *Physics Department, Rensselaer Polytechnic Institute, Troy, NY 12180, USA*

[11] *Institute of High Energy Physics, Chinese Academy of Sciences, Beijing 100049, P.R. China*

Contents

Abstract

This document outlines major directions in theoretical support for the measurement of nucleon resonance transition form factors at the JLab 12 GeV upgrade with the CLAS12 detector. Using single and double meson production, prominent resonances in the mass range up to 2 GeV will be studied in the range of photon virtuality Q^2 up to 12 GeV^2 where quark degrees of freedom are expected to dominate. High level theoretical analysis of these data will open up opportunities to understand how the interactions of dressed quarks create the ground and excited nucleon states and how these interactions emerge from QCD. The paper reviews the current status and the prospects of QCD based model approaches that relate phenomenological information on transition form factors to the non-perturbative strong interaction mechanisms, that are responsible for resonance formation.

I. INTRODUCTION

Nucleons and baryons in general, have played an essential role in the development of our understanding of the strong interaction. The concept of quarks was first made manifest through the study of baryon spectroscopy, which subsequently led to the development of dynamical constituent quark models (CQMs) in the late 1960's [1] and further developed in the 1970's [2, 3]. As a result of intense experimental and theoretical effort, especially in recent years, it has become clear that the structure of the nucleon and its excited states (Δ^* and N^*) is much more complex than what can be described in terms of constituent quarks only. The structure of low-lying baryon states, as revealed by electromagnetic probes at low momentum transfer, can be described reasonably well by adding meson-baryon effects phenomenologically to the predictions from constituent quark models [4, 5, 6, 7, 8, 9, 10]. However, a fundamental understanding of the properties of the nucleon and its excited states at short distances, which are accessible using probes with sufficiently high momentum transfer, demands the full machinery of Quantum Chromodynamics (QCD). In recent years, there has been tremendous progress in this direction. Constituent quark models have been greatly refined by using fully relativistic treatments [5, 6, 7, 8] and by including sea quark components [11, 12, 13]. The hypercentric CQM with improved treatment of constituent quark interactions [9, 10] has emerged. A covariant model based on the Dyson-Schwinger equations [14] (DSE) of QCD is now emerging as a well-tested and well-constrained tool to interpret baryon data directly in terms of current quarks and gluons. This approach also provides a link between the phenomenology of dressed current quarks and Lattice QCD (LQCD). Relations between baryon transition form factors and the Generalized Parton Distributions (GPDs) have also been formulated [15, 16] that connect these two different approaches to describing baryon structure. On a fundamental level, Lattice QCD is progressing rapidly in making contact with the excited baryon data. The USQCD Collaboration, involving JLab's LQCD group, has been formed to perform calculations for predicting the baryon spectrum and $\gamma_v NN^*$ transition form factors.

On the experimental side, extensive data on electromagnetic meson production have been obtained at JLab, MIT-Bates, LEGS, MAMI, ELSA, and GRAAL in the past decade. The analyses of these data and the data expected in the next few years before the start of experiments with the JLab 12-GeV upgrade, will resolve some long-standing problems in

baryon spectroscopy and will provide new information on the structure of N^* states. To enhance this effort, the Excited Baryon Analysis Center (EBAC) was established in 2006 and is now making rapid progress in this direction. Analysis models developed at Mainz, JLab, GWU, and Bonn are also being greately refined to analyze the recent data. Significant progress from this experiment-theory joint effort has been made in the past few years.

With the 12 GeV upgrade of CEBAF at JLab and the development of experimental facilities at Mainz and Bonn, new opportunities for investigating the spectrum and structure of excited baryon states will soon become available. To develop research programs for this new era, a workshop on Electromagnetic $\gamma_v NN^*$ Transition Form Factors was held at Jefferson Laboratory, October 13-15, 2008 [17]. The main objectives of the workshop were (a) to review the status of the $\gamma_v NN^*$ transition form factors extracted from the meson electroproduction data, and (b) to call for the theoretical interpretations of the extracted N-N^* transition form factors, that enable access to the mechanisms responsible for the N* formation and to their emergence from QCD.

This document summarizes the contributions of workshop participants that provide theoretical support for the excited baryon program at the 12 GeV energy upgrade at JLab.

II. PHYSICS FROM LATTICE QCD

Quantum Chromodynamics (QCD), when combined with the electroweak interactions, underlies all of nuclear physics, from the spectrum and structure of hadrons to the most complex nuclear reactions. Lattice gauge calculations enable the *ab initio* study of many of the low-energy properties of QCD. There are significant efforts underway internationally to use lattice QCD to directly compute properties of the ground and excited state nucleon and, generically, the baryon spectrum of matter, including spectrum and structure.

The Hadron Spectrum Collaboration involving the Lattice Group at Jefferson Lab, Carnegie Mellon University, Univ. of Maryland, and Trinity College (Dublin) has embarked on an ambitious program to compute the high lying excited state spectrum of baryons and mesons, as well as their (excited state) electromagnetic transition form-factors up to $Q^2 \sim 10$ GeV^2. A particularly important quantity to compute is the photo-coupling value for exotic mesons which is of relevance for experiments in the future Hall D at JLab. With the new techniques that will be used to extract resonance information, it is intended that the

spectrum and couplings that are determined can be used to provide valuable comparisons with experimental data, and provide input for programs like EBAC.

There are several key technologies needed in this campaign. To adequately resolve excited state energies and to keep the calculational costs manageable, an anisotropic lattice formulation is used with three flavors of quarks - two light and a strange quark. These new type of lattices require a significant amount of computing resources since previous lattice configurations cannot be (re)used. As described in Ref. [18], a successful program is underway to generate these lattices using DOE and NSF computing resources, and those available within the USQCD collaboration, including clusters at JLab. It is anticipated that the production of configurations at the *physical* pion mass will proceed early in 2009 using the next generation of Cray supercomputers at ORNL.

Another key component in the hadron spectrum campaign is the use of variational techniques for constructing correlators. The hadron creation operators used in the correlators should have significant overlap with the hadron states of interest. In Ref. [19], group theoretical techniques have been used to construct non-local interpolating fields that characterize possible hadron states. Their spins are classified according to irreducible representations of the cubic rotation group – the remnants of the rest frame Lorentz group when discretized. These large bases of operators are used in a variational calculation which allows for the extraction of a large number of excited states. In Figure 1 is shown the extracted energies of highly excited levels of the nucleon spectrum at unphysical pion masses using two flavors of anisotropic quarks [20]. The technique to reconstruct the continuum spin states which are broken into lattice irreducible representations has been developed in Ref. [21]. These techniques are being used now in light quark mass calculations of the baryon spectrum as well as the meson spectrum over the $N_f = 2 + 1$ configurations.

At large enough quark mass, the ground and probably many of the excited baryon states are stable under the strong interactions. However, as the quark mass decreases, decay channels open up which are of lower energy compared to the state of interest. A critically key component in this hadron spectrum campaign is identifying how these single particle and multi-particle states shift with changes in the physical volume of the lattice. These finite volume techniques, developed by Lüscher, have successfully been used in mesonic systems, but their use in baryonic systems is relatively new and are actively under investigation.

From the excited energies of the nucleon spectrum, one can compute electromagnetic

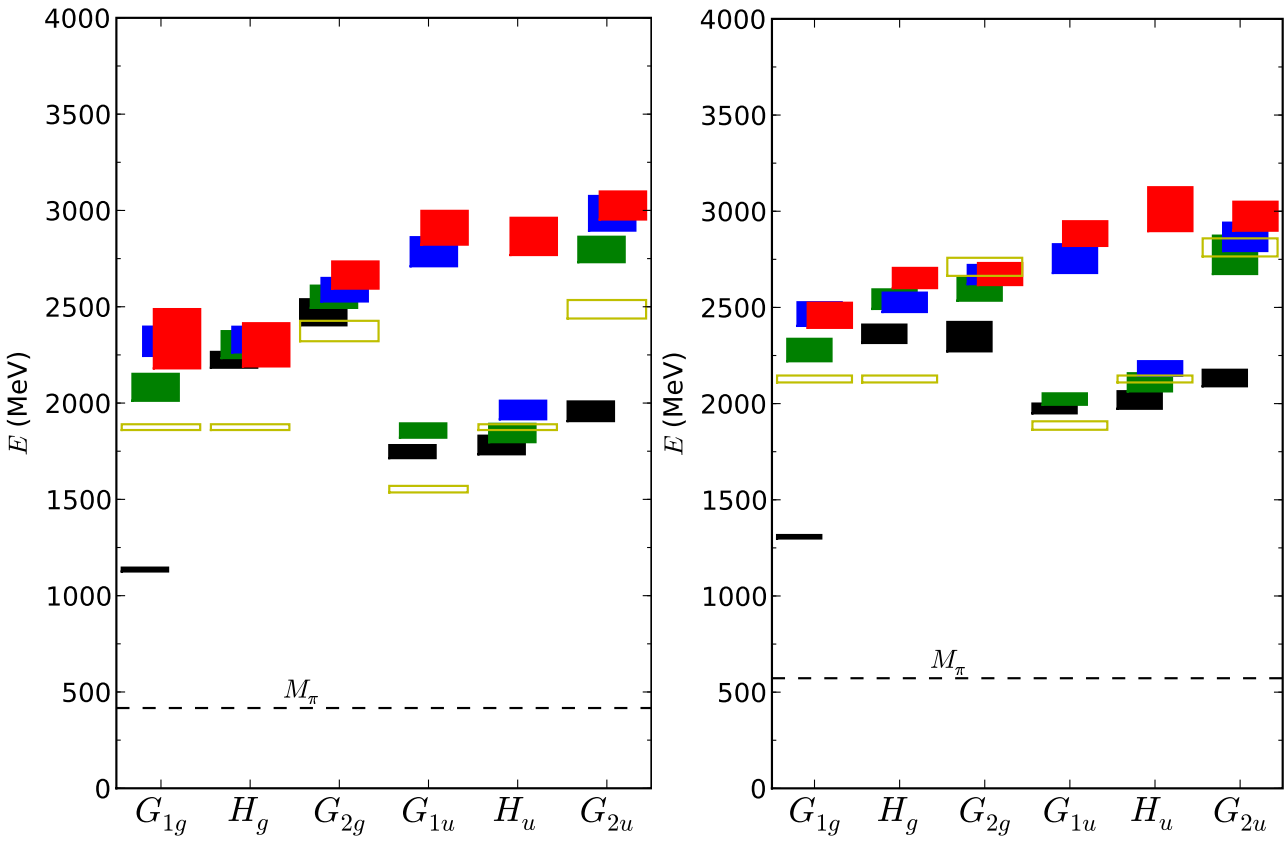

FIG. 1: The energies obtained for each symmetry channel of isospin $\frac{1}{2}$ baryons are shown based on the $2.64fm^3$ $N_f = 2$ lattice QCD data for $m_\pi = 400$ MeV (left panel) and $m_\pi = 572$ MeV (right panel). The scale shows energies in Mev and errors are indicated by the vertical size of the box. The gold open boxes show $N\pi$ threshold states.

form-factors. First exploratory results have been obtained in Ref. [22] for the excited nucleon $P_{11} - N$ transition using a very simple basis of operators. The main result is shown in Figure 2. The low Q^2 region for $F_2(Q^2)$, at these very large unphysical pion masses shows large deviations from experiment, consistent with many statements that the pion cloud effects are stronger in excited state systems compared to the ground states. However, these first preliminary results are very encouraging given the very limited operator basis. Work is underway now using the previously developed full basis of nucleon operators for a more accurate computation of the excited nucleon form-factors at much smaller pion masses using the $N_f = 2 + 1$ configurations already produced. In addition, the ground and excited state hyperon transition form-factors will also be computed. It is not clear what kind of statistical accuracy that might be achieved - it is very sensitive to the system of interest, what excited level, and what Q^2 (many are available in one calculation). The results in

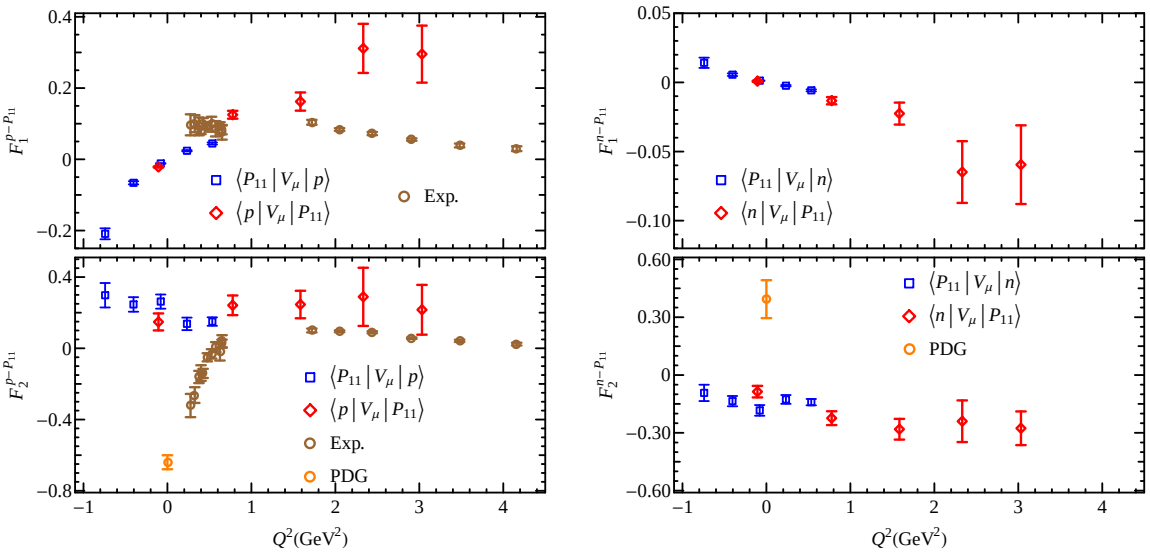

FIG. 2: Left panel: proton-Roper form factors $F^*_{1,2}$ obtained from CLAS experiments and PDG number (circles) and lattice methods (squares, diamonds). Right panel: neutron-Roper form factors $F^*_{1,2}$ obtained from PDG number (circles) and lattice methods (squares, diamonds)

Fig. 2 are illustrative.

The Q^2 range in these current form-factor calculations is typically up to about 3 to 4 GeV^2. To go to about 10 GeV^2 requires some different techniques. One method is to go to smaller lattice spacing a where $Q^2 \sim 1/a^2$. Since more than one lattice spacing is needed for continuum extrapolations, this change will happen, probably in late 2009. However, a more immediate method involves going to the (anti)-Breit frame between the initial and final nucleon states, whereby the Q^2 is maximized. Using this technique (Ref. [23]), the previous calculation for the $P_{11} - N$ transition was extended up to 6 GeV^2, again at unphysically large pion masses, and it seems feasible to go somewhat higher Q^2. This (anti)-Breit frame technique is being used in lighter pion mass calculations. As the pion mass decreases, the previous results at time-like Q^2 will slide to larger (positive) values, and hence the Q^2_{max} values will also increase to greater than 7 GeV^2. Again, the obtainable statistical error in this large Q^2 region is not known at this time.

In parallel with this work of the computation of the excited nucleon spectrum, significant effort is going into the calculation of the excited meson spectrum. First efforts (Ref. [21]) have gone into an extensive calculation of the excited charmonium spectrum. The goal of this work is the determination of the charmonium version of the 1^{-+} photo-coupling as

phenomenological input for GlueX. Working is proceeding now on the calculation of the 1^{-+} photocoupling at the strange quark mass scale, and soon for the light quark mass scale.

III. CHARTING THE INTERACTION BETWEEN LIGHT QUARKS

Two of the basic motivations for an upgraded JLab facility are the needs: to determine the essential nature of light-quark confinement and dynamical chiral symmetry breaking (DCSB); and to understand nucleon structure and spectroscopy in terms of QCD's elementary degrees of freedom. In addressing these questions one is confronted with the challenge of elucidating the role of quarks and gluons in hadrons and nuclei. In accepting that challenge one steps immediately into the domain of relativistic quantum field theory where within the key phenomena can only be understood via nonperturbative methods.

It is a fundamental fact that the physics of hadrons is dominated by two *emergent phenomena*: confinement; namely, the empirical truth that quarks have not hitherto been detected in isolation; and DCSB, which is responsible, amongst many other things, for the large mass splitting between parity partners in the spectrum of light-quark hadrons, even though the relevant current-quark masses are small. Neither of these phenomena is apparent in QCD's Lagrangian and yet they play a principal role in determining the observable characteristics of real-world QCD.

In connection with confinement it is worth emphasizing at the outset that the potential between infinitely-heavy quarks measured in numerical simulations of quenched lattice-regularised QCD – the so-called static potential – is simply not relevant to the question of light-quark confinement. In fact, it is quite likely a basic feature of QCD that a quantum mechanical potential between light-quarks is impossible to speak of because particle creation and annihilation effects are essentially nonperturbative. A perspective on confinement was laid out in Ref. [24]. Expressed simply, confinement can be related to the analytic properties of QCD's Schwinger functions, which are often loosely called Euclidean-space Green functions. For example, it can be read from the reconstruction theorem that the only Schwinger functions which can be associated with expectation values in the Hilbert space of observables; namely, the set of measurable expectation values, are those that satisfy the axiom of reflection positivity [25]. This is an extremely tight constraint. However, it is a necessary but not sufficient condition.

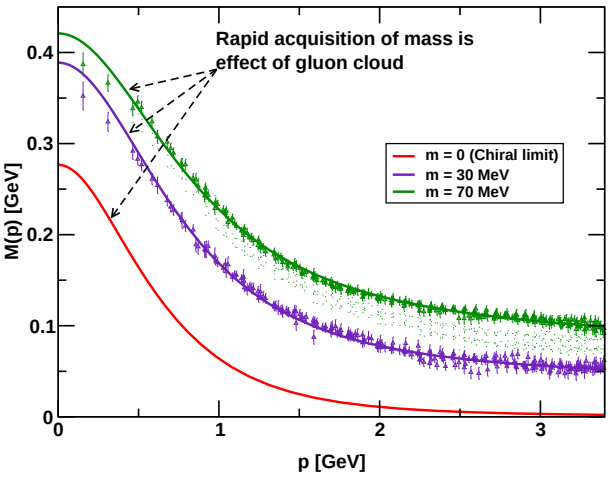

FIG. 3: *Dressed-quark mass function, $M(p)$: solid curves – DSE results [28, 29], "data" – numerical simulations of unquenched lattice-QCD [30]. In this figure one observes the current-quark of perturbative QCD evolving into a constituent-quark as its momentum becomes smaller. The constituent-quark mass arises from a cloud of low-momentum gluons attaching themselves to the current-quark. This is dynamical chiral symmetry breaking: an essentially nonperturbative effect that generates a quark mass* from nothing*; namely, it occurs even in the chiral limit.*

The question of light-quark confinement can be translated into that of charting the infrared behavior of QCD's *universal* β-function. It is important to appreciate that while this function may depend on the scheme chosen to renormalize the quantum field theory, it is unique within a given scheme. An elemental goal of hadron physics during the next ten years must be to design a program of experiment and theory that can together map out the β-function. This is a well-posed problem. It's importance is already widely appreciated and an exploratory attempt has been made [26].

While light-quark confinement remains a conjecture, many statements of fact can be made in connection with DCSB. For example, DCSB explains the origin of constituent-quark masses and underlies the success of chiral effective field theory. Understanding DCSB within QCD proceeds from the renormalised gap equation [27]:

$$S(p)^{-1} = Z_2\,(i\gamma\cdot p + m^{\rm bm}) + Z_1 \int_q^\Lambda g^2 D_{\mu\nu}(p-q)\frac{\lambda^a}{2}\gamma_\mu S(q)\Gamma^a_\nu(q,p)\frac{d^4q}{(2\pi)^4}, \qquad (1)$$

where $\int_q^\Lambda$ represents a Poincaré invariant regularisation of the integral, with Λ the regularisation mass-scale, $D_{\mu\nu}$ is the renormalised dressed-gluon propagator, Γ_ν is the renormalised dressed-quark-gluon vertex, and $m^{\rm bm}$ is the quark's Λ-dependent bare current-mass. The vertex and quark wave-function renormalisation constants, $Z_{1,2}(\zeta^2,\Lambda^2)$, depend on the gauge parameter.

The solution to Eq. (1) has the form

$$S(p) \;=\; -i\gamma\cdot p\,\sigma_V(p^2,\zeta^2) + \sigma_S(p^2,\zeta^2) = \frac{1}{i\gamma\cdot p\,A(p^2,\zeta^2) + B(p^2,\zeta^2)} = \frac{Z(p^2,\zeta^2)}{i\gamma\cdot p + M(p^2)} \qquad (2)$$

and it is important that the mass function, $M(p^2) = B(p^2,\zeta^2)/A(p^2,\zeta^2)$ is independent of the renormalisation point, ζ.

The dressed-quark mass function in QCD is depicted in Fig. 3. It is one of the most remarkable features of the theory. In perturbation theory it is impossible in the chiral limit to obtain $M(p^2) \neq 0$: the generation of mass *from nothing* is an essentially nonperturbative phenomenon. On the other hand, it is a longstanding prediction of nonperturbative DSE studies that DCSB will occur so long as the integrated infrared strength possessed by the gap equation's kernel exceeds some critical value [31]. There are strong indications that this condition is satisfied in QCD [28, 29, 30]. It follows that the quark-parton of QCD acquires a momentum-dependent mass function, which at infrared momenta is $\sim$ 100-times larger than the current-quark mass. This effect owes primarily to a dense cloud of gluons that clothes a low-momentum quark [32]. It means that the Higgs mechanism is largely irrelevant to the bulk of normal matter in the universe. Instead the single most important mass generating mechanism for light-quark hadrons is the strong interaction effect of DCSB; e.g., one can identify it as being responsible for 98% of a proton's mass.

It is widely anticipated that there is an intimate connection between DCSB and light-quark confinement. For example, analogous to quenched QCD, quenched QED in three dimensions (two spacial, one temporal – QED_3) is confining because it has a nonzero string tension [33]. The effect of unquenching; viz., allowing light fermions to influence the theory's dynamics, has been much studied. The nature of QED_3 is such that there is almost certainly a critical number of light flavors above which DCSB is impossible. Moreover, chiral symmetry restoration and deconfinement are coincident owing to an abrupt change in the analytic properties of the fermion propagator when a nonzero scalar self-energy becomes insupportable [34].

The complex of Dyson-Schwinger equations (DSEs) is a powerful tool that has been employed with marked success to study confinement and DCSB, and their impact on hadron observables [31, 35, 36, 37, 38]. Moreover, the existence of a nonperturbative and symmetry preserving truncation scheme [39, 40, 41, 42] has enabled the DSEs to be used to provide an explanation of dynamical chiral symmetry breaking and prove a body of exact results for pseudoscalar mesons [27, 43]. They relate even to radial excitations and/or hybrids [44, 45, 46], and heavy-light [47, 48] and heavy-heavy mesons [49]. Mesons are described by the fully covariant Bethe-Salpeter equation and the exact results have been illustrated using a

renormalisation-group-improved ladder-rainbow truncation of this and the gap equation [43, 50], which also provided a prediction of the electromagnetic pion form factor [51]. (Ladder-rainbow is the leading-order DSE truncation.) In addition, algebraic parametrizations of the dressed-quark propagators and meson bound-state amplitudes obtained from such studies continue to be useful, in particular with the study of B-meson $\to$ light-meson transition form-factors [52] and baryon properties [53, 54, 55, 56].

In quantum field theory a baryon appears as a pole in a six-point quark Green function. The residue is proportional to the baryon's Faddeev amplitude, which is obtained from a Poincaré covariant Faddeev equation that sums all possible exchanges and interactions that can take place between three dressed-quarks. A tractable Faddeev equation for baryons was formulated in Ref. [57]. It is founded on the observation that an interaction which describes colour-singlet mesons also generates quark-quark (diquark) correlations in the colour-$\bar{3}$ (antitriplet) channel [58]. The lightest diquark correlations appear in the $J^P = 0^+, 1^+$ channels and hence only they are retained in approximating the quark-quark scattering matrix. While diquarks do not appear in the strong interaction spectrum; e.g., Refs. [40, 41, 42], the attraction between quarks in this channel justifies a picture of baryons in which two quarks are always correlated as a colour-$\bar{3}$ diquark pseudoparticle, and binding is effected by the iterated exchange of roles between the bystander and diquark-participant quarks.

The Poincaré covariant and quantum field theoretical DSE framework is well suited to addressing the question of light-quark confinement. It may be posed as the problem of developing a detailed understanding of the infrared evolution of the quark-quark scattering kernel, $K_{q\bar{q}}$. With Refs. [59, 60] significant progress has been made in this direction. They enable the direct correlation of meson and baryon properties via a single interaction kernel that preserves QCD's one-loop renormalisation group behaviour and can systematically be improved. The unified framework provides a veracious description of the pion as both a Goldstone mode and a bound state of dressed-quarks. It is the only approach that is capable of doing so because it alone is capable of expressing the behavior in Fig. 3. The studies predict, amongst other things, the evolution of the nucleon mass with a quantity that can methodically be connected with the current-quark mass in QCD. This is depicted in Fig. 4. Notably, the nucleon mass is insensitive to the kernel's single parameter despite the large dependence of the unobservable diquark masses. Systematic corrections to the DSE's leading order truncation have been shown to move results into line with experiment.

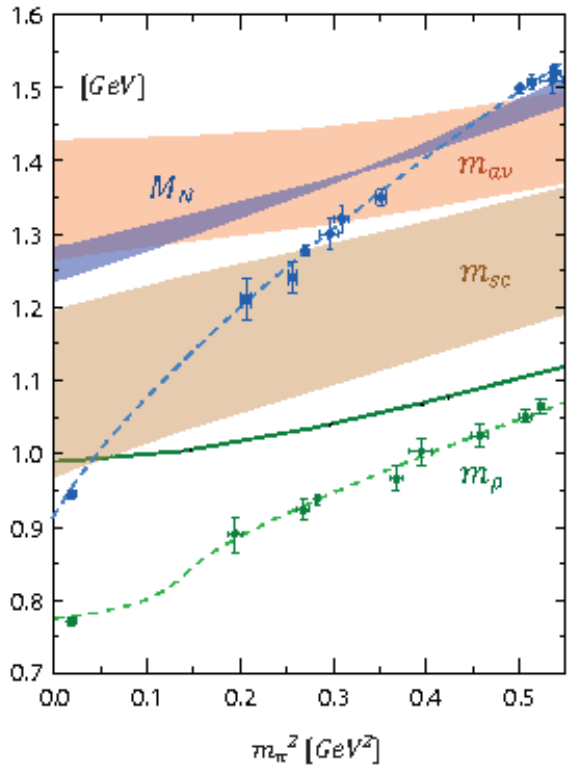

FIG. 4: *Thick bands*: Evolution with current-quark mass, $\hat{m}$, of the scalar and axial-vector diquark masses: m_{sc} and m_{av}. Bands demarcate sensitivity to the variation in ω: $r_a = 1/\omega$ can be associated with a confinement length-scale in the quark-quark scattering kernel. (m_π, calculated from rainbow-ladder meson Bethe-Salpeter equation: $\hat{m} = 6.1\,\text{MeV} \Rightarrow m_\pi = 0.138\,\text{GeV}$.) *Solid curve*: Evolution of ρ-meson mass [59]. This observable quantity is insensitive to ω. With m_ρ, results from simulations of lattice-regularised QCD [61] are also depicted along with an analysis and chiral extrapolation [62], *short dashed curve*. *Thin band*: Evolution with $\hat{m}$ of the nucleon mass obtained from the Faddeev equation: $\hat{m} = 6.1\,\text{MeV}$, $M_N = 1.26(2)\,\text{GeV}$ cf. results from lattice-QCD [63, 64] and an analysis of such results [65], *dashed curve*. (Figure adapted from Ref. [60].)

An international theory program is underway that exploits the strengths of the DSEs in studies of the spectrum and interactions of hadrons. In connection with this, a comprehensive study of nucleon electromagnetic form factors has just been completed [66]. It evaluates a dressed-quark core contribution, which is defined by the solution of a Poincaré covariant Faddeev equation in which dressed-quarks provide the elementary degree of freedom and correlations between them are expressed via diquarks. The diquarks are nonpointlike and the current depends on their charge radii. A particular feature of the study is a separation of form factor contributions into those from different diagram types and correlation sectors, and subsequently a flavour separation for each of these. Amongst the extensive body of results that one might highlight: $r_1^{n,u} > r_1^{n,d}$, owing to the presence of axial-vector quark-quark correlations; and for both the neutron and proton the ratio of Sachs electric and magnetic form factors possesses a zero.

The latter ratios are depicted in Fig. 5. A sensitivity to the nucleon's electromagnetic current is evident, here expressed via the diquarks' radius. However, irrespective of that radius, the electric form factors possess a zero and the magnetic form factor is positive definite. On $Q^2 \lesssim 3\,\text{GeV}^2$ the proton result lies below experiment. As explained in Ref. [66],

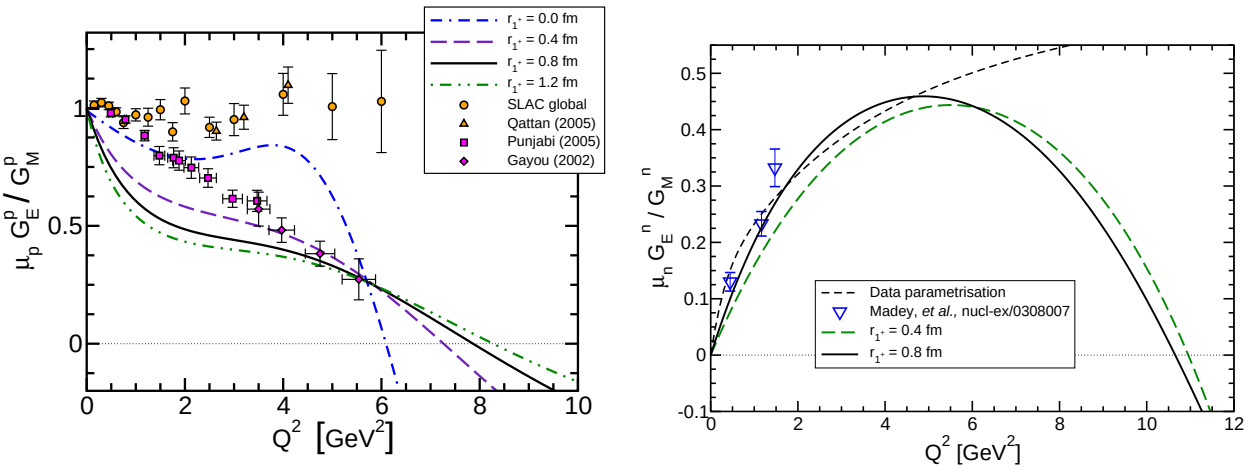

FIG. 5: *Left panel* – Result for the normalised ratio of proton Sachs electric and magnetic form factors computed with four different diquark radii. Data: diamonds – [67]; squares – [68]; triangles – [69]; and circles [70]. *Right panel* – Analogous ratio for the neutron computed with two different diquark radii. *Short-dashed curve*: parametrisation of Ref. [71]. *Down triangles*: data from Ref. [72].

this can likely be attributed to omission of so-called pseudoscalar-meson-cloud contributions.

It has long been recognized that the behavior characterized by Fig. 3 has an enormous impact on hadron phenomena [73] and hence that a form factor's pointwise evolution with momentum transfer is a sensitive probe of the nature of the quark-quark scattering kernel. For example, this was made strikingly apparent for the pion in Ref. [74]. It can also be seen for the nucleon. In the left panel of Fig. 6 we depict the proton's Pauli form factor calculated in a confining Nambu–Jona-Lasinio model, whose simplicity and phenomenological efficacy has recently been much exploited [75, 76, 77, 78]. This model possesses a dressed-quark mass but it *does not run*; i.e., it assumes a large value that is momentum independent. As apparent in the figure, in this case the agreement between model result and experiment deteriorates quickly with increasing momentum transfer and the ultraviolet power-law behavior is incorrect. This may be contrasted with the behavior in the right panel, which is obtained [66] using a momentum-dependent running quark mass of the type depicted in Fig. 3. This calculation omits the pseudoscalar meson cloud. However, it retains the fully momentum dependent dressed-quark structure, which ensures good agreement with data for $Q^2 \approx 2-3M_N^2$.

We judge that it is possible to employ precision data on nucleon-resonance transition form factors as a means by which to chart the momentum evolution of the dressed-quark

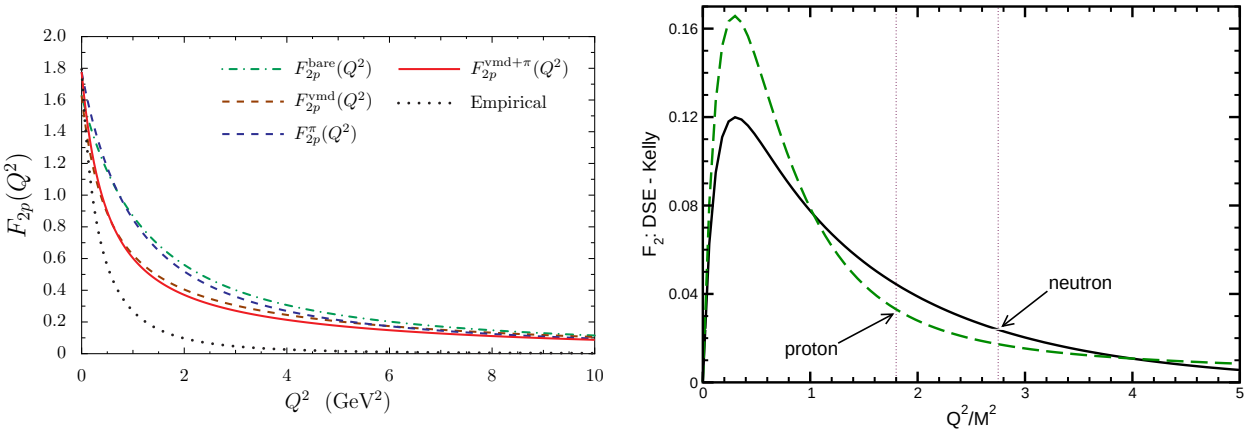

FIG. 6: *Left panel* – Confining-NJL model Faddeev equation result for the proton's Pauli form factor: *solid curve*, complete result; and *dotted curve*, parametrization of experimental data [71]. The curves labelled *bare*, *VMD* and π represent intermediates stages in the calculation of the solid curve. *Right panel* – Difference between a DSE-calculated dressed-quark core contribution to the Pauli form factor and a parametrisation of experimental data [71], each normalised by the appropriate anomalous magnetic moment at $Q^2 = 0$: *dashed curve* – proton; *solid curve* – neutron. At $Q^2 \approx 2M_N^2$ the difference between calculation and data in the *left panel* is an order of magnitude larger than in the *right panel*.

mass function and therefrom the infrared behavior of QCD's β-function; in particular, to locate unambiguously the transition boundary between the constituent- and current-quark domains that is signaled by the sharp drop apparent in Fig. 3. That can be related to an inflexion point in QCD's β-function. Contemporary theory indicates that this transition boundary lies at $p^2 \sim 0.6\,\mathrm{GeV}^2$. Since a probe's input momentum Q is principally shared equally amongst the dressed-quarks in a transition process, then each can be considered as absorbing a momentum fraction $Q/3$. Thus in order to cover the domain $p^2 \in [0.5, 1.0]\,\mathrm{GeV}^2$ one requires $Q^2 \in [5, 10]\,\mathrm{GeV}^2$.

An international theory effort is underway in order to realize the goal of turning experiment into a probe of the dressed-quark mass function. The effort has many facets and the first calculations are being performed at leading-order in the DSE truncation.

Naturally, a reference calculation is needed, one that does not incorporate the running of the dressed-quark mass which is such a singular feature of QCD. A calculation of this type is nearing completion [79] and a preliminary result is presented in Fig. 7. It is evident that the pion is playing a very important role but significant strength is missing in the neighborhood of $Q^2 = 0$, since empirically $G_M(Q^2 = 0) = 3$. This calculation must be analyzed and the origin of each feature and defect determined so that the role of a constant constituent-quark-

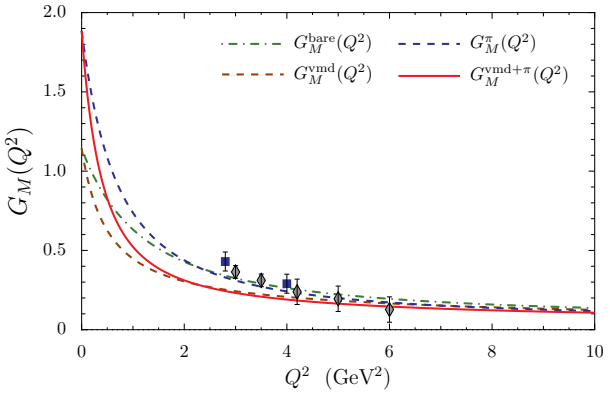

FIG. 7: *Solid curve* – Confining-NJL model Faddeev equation result for the $N \to \Delta$ M1 transition form factor, complete calculation. The curves labelled *bare*, *VMD* and π represent intermediates stages in the calculation. Data from Refs. [80, 81].

like mass can unambiguously be identified. The analysis should be complete by mid-2009.

Following this effort the Faddeev equation framework of Refs. [53, 54, 55, 56, 66], described briefly above and widely employed in studies of nucleon and Δ properties, will be applied to the $N \to \Delta$ transition. The strong momentum dependence of the dressed-quark mass function is an integral part of this framework. Therefore, in this study it will be possible, e.g., to vary artificially the position of the marked drop in the dressed-quark mass function and thereby identify experimental signatures for its presence and location. This study would begin in 2010 and be completed by the end of that year.

In parallel with these efforts, the *ab-initio* rainbow-ladder DSE framework of Refs. [59, 60] is being extended to the Δ resonance. A solution of the Faddeev equation for the Δ should be complete by the end of 2010 [82]. The nucleon-photon current developed in Ref. [60] will then be generalized so that its nucleon form factor studies can be correlated with a calculation of the $N \to \Delta$ transition. The time required to complete this effort is uncertain, given that it involves a PhD student who is now nearing completion of his research, but assuming that a new student is found or a postdoctoral fellow can assume responsibility, a reasonable estimate is for completion by the end of 2010. It should be emphasized, however, that for technical reasons this effort can only produce form factors out to modest momentum transfer; viz., $Q^2 \sim 2\,M_N^2$.

In order to extend the calculations it is imperative to improve the numerical methods used in the calculation of form factors and also to improve the rainbow-ladder quark-quark scattering kernel. This is naturally part of the next phase of the theoretical effort.

One should also proceed beyond the leading-order DSE truncation. This is necessary in order to identify and isolate artefacts that may arise through truncation and their impact on predictions for experimental signatures of the transition between the constituent-quark

and the current-quark domains. This need notwithstanding, the merits of the rainbow-ladder truncation should not be underestimated. It is exact for $p^2 \gtrsim 1\,\mathrm{GeV}^2$. Furthermore, contemporary estimates show that at smaller p^2 it is still semi-quantitatively accurate for a wide range of observables, the nature of which can be determined *a priori*. Careful application of the rainbow-ladder truncation yields insights that are generally reliable.

A path for proceeding beyond the rainbow-ladder truncation is charted. Owing to the relative ease of dealing with the Bethe-Salpeter equation, it will initially proceed via mesons. The one-parameter model for the infrared behavior of $K_{q\bar{q}}$ in Ref. [59] will be employed in in DSE calculations of the spectrum and interactions of pseudoscalar mesons with masses $< 2\,\mathrm{GeV}$. Comparison with scant extant data will inform improvements of the *Ansatz*, as will continuing DSE and lattice-QCD research on the pointwise behavior of the dressed-quark-gluon vertex. It is in a nontrivial vertex that one moves beyond the rainbow-ladder truncation.

The improved $K_{q\bar{q}}$ will be employed in studies of the spectrum and interactions of axial-vector mesons, all of which lie above 1 GeV. The properties of pseudoscalar excited states and axial-vector mesons are a sensitive probe of the long-range part of the interaction between light-quarks. Comparison with scarce data will assist in further improving the map of the light-quark confinement interaction. A well constrained form of $K_{q\bar{q}}$ will thereafter be available. It will enable reliable predictions for the properties of all mesons in the $1-2\,\mathrm{GeV}$ range, including hybrids and exotics. This extended kernel will provide the basis for future *ab initio* Faddeev equation studies of the nucleon and Δ. One may anticipate that those studies could begin in 2013.

In the meantime, following the successful completion of $N \to \Delta$ studies, the dressed-quark Faddeev equation will be employed in nucleon resonance spectroscopy and the calculation of additional nucleon to resonance transitions. The starting point for this effort will be a calculation of the dressed-quark component of the Roper resonance. With experiment [8] now pointing to an interpretation of the $N(1440)$ as a radial excitation of the nucleon, a compelling case can be made for employing a quantum field theoretical approach to QCD that is founded on dressed-quark degrees of freedom in order to determine whether the experimental claim is consistent with the best available theory. A conclusion on this point should be available from the DSE-based Faddeev equation by the end of 2011 and from the *ab initio* rainbow-ladder truncation by 2012.

In parallel with the program outlined here an effort will be underway at the Excited Baryon Analysis Center (EBAC), which will provide the reaction theory necessary to make reliable contact between experiment and predictions based on the dressed-quark core. While rudimentary estimates can and will be made of the contribution from pseudoscalar meson loops to the dressed-quark core of the nucleon and its excited states, a detailed comparison with experiment will only follow when the DSE-based results are used to constrain the input for dynamical coupled channels calculations.

IV. ELECTROPRODUCTION OF N^* RESONANCES AT LARGE MOMENTUM TRANSFERS

Form factors play an extremely important role in the studies of the internal structure of composite particles as the measure of charge and current distributions. In particular transitions to nucleon excited states allow to study the relevant degrees of freedom, wave function and interaction between the constituents, and the transition to pQCD. The prediction of QCD is that at large momentum transfers the form factors become increasingly dominated by the contribution of the valence state with small transverse separation between the quarks. There is a growing consensus that the ultimate pQCD picture based on hard rescattering involving two gluon exchanges is not achieved at present energies; however, at photon virtualities from 5 to 10 GeV^2 of CLAS12 we will have access to quark degrees of freedom, whereas the description in terms of meson-baryon degrees of freedom becomes much less suitable than at smaller momentum transfers.

The major challenge for theory is that quantitative description of form factors in this region must include soft nonperturbative contributions. An approach that is most directly connected to QCD is based on the light-cone sum rules (LCSRs) [83, 84]. This technique allows one to calculate form factors using much more limited information compared to the full nonperturbative wave functions, albeit with some assumptions. The LCSRs are derived from the correlation function of the type

$$\int dx\, e^{-iqx} \langle N^*(P)|T\{\eta(0) j_\mu^{\rm em}(x)\}|0\rangle \tag{3}$$

where η is a suitable operator with nucleon quantum numbers. More detail can be found

in the following contribution to these proceedings (Ref. [85]). Making use of the duality of QCD quark-gluon and hadronic degrees of freedom through dispersion relations one can write a representation for the transition form factors in terms of the N^* momentum fraction distributions of partons at small transverse separations in the N^*, dubbed distribution amplitudes (DAs) which are the same quantities that enter the pQCD calculation, cf. [86, 87]. The LCSRs provide one with the most direct relation of the hadron form factors and DAs that is available at present, with no other nonperturbative parameters.

The necessary information on the DAs can be obtained from LQCD. The theoretical particle and nuclear physics group in Regensburg is a member of QCDSF and the SFB/Transregio 55 "Hadron Physics with Lattice QCD" which is a large-scale research program aimed at the study of hadron structure using LQCD techniques. The studies of hadron DAs present one of the long-term goals of this collaboration and they will be continued. The most important steps so far have been the calculation of the second moment of the pion DA [88], the classification of three-quark operators in irreducible spinor respresentations of the hypercubic group [89], the calculation of nonperturbative renormalization constants for three-quark operators [90] and the evaluation of the lowest moments of the DAs of the nucleon [91] and its parity partner $N^*(1535)$ [92]. According to our preliminary study, quark distributions in the nucleon and $N^*(1535)$ are rather different, see Fig. 8.

We find a larger wave function of the three quarks at the origin in the $J^P = \frac{1}{2}^-$ state compared to $J^P = \frac{1}{2}^+$ state that may be counterintuitive. The momentum fraction carried by the u-quark with the same helicity as the baryon itself appears to be considerably larger for N^* resonance, indicating that its DA is more asymmetric. The future plans are, first of all, to repeat the same calculations with smaller pion masses and larger lattices that are expected to become available within 2-3 years. This would remove a major source of uncertainties which is due to the chiral extrapolation. Second, we want to expand our calculation of the moments of the DAs to the whole $J^P = 1/2^+$ and $J^P = 1/2^-$ baryon octets and later also to the decuplet. We will also explore possibilities to calculate higher moments of DAs and also moments of the generalized parton distributions involving different hadrons in the initial and final state (sometimes referred to as TDAs). All such calculations will require a dedicated effort, and the accuracy of the predictions may vary.

The results of the LCSR calculation of the helicity amplitides of the electroproduction of $N^*(1535)$ using LCQD input on the DA are presented in Fig. 9. This calculation corresponds

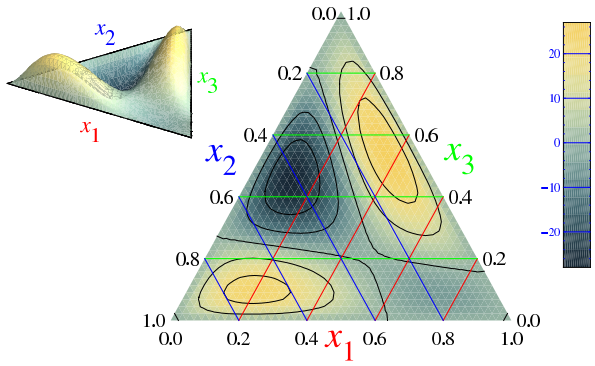

(a)

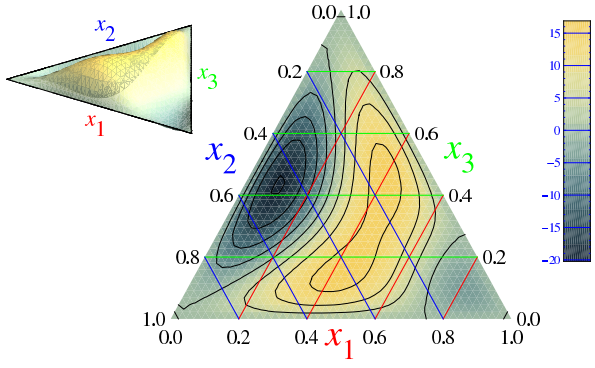

(b)

FIG. 8: Barycentric plot of the distribution amplitudes for nucleon (a) and $N^\star(1535)$ (b) at $\mu_{\overline{MS}} = 1$GeV [92]. The lines of constant x_1, x_2 and x_3 are parallel to the sides of the triangle labelled by x_2, x_3 and x_1, respectively.

to the simplest, tree-level (or leading-order) LCSRs The errors on the parameters of the DAs induce an uncertainty in the calculation of the form factors of order 30%. This can be reduced in the future. In addition, using quark-hadron duality in the identification of the nucleon contribution, which is endemic to the LCSR approach, introduces an irreducible uncertainty of the order of 10-20% in the whole Q^2 range. In the region $Q^2 > 2$ GeV^2 where the light-cone expansion may be expected to converge, the results appear to describe the general features of the data rather well. The small $S_{1/2}$ amplitude arises as a result of strong cancellations between contributions of the helicity conserving and helicity violating form factors and is difficult to predict reliably. The shown uncertainty is likely to be underestimated for this case.

The LCSR approach is rather general; it has been applied e.g. to the $N\gamma\Delta$ transitions [93] and to threshold pion electroproduction [94, 95]. In all cases, however, the LCSRs of the type considered here cannot be extended below $Q^2 \sim 1$ GeV^2 because of the so-called

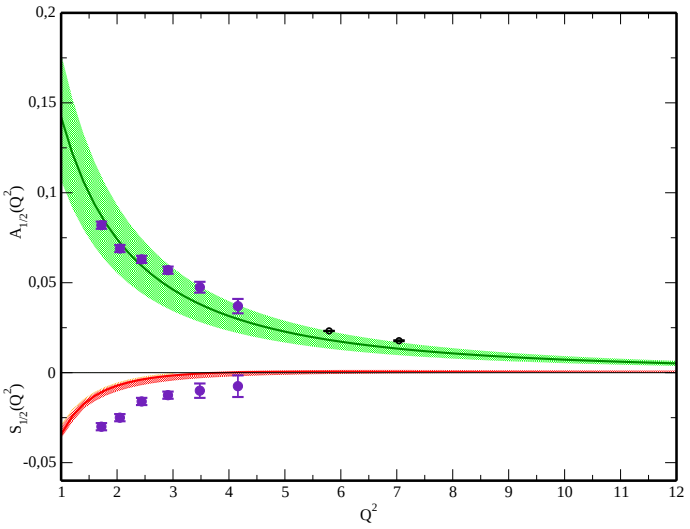

FIG. 9: The LCSR calculation for the helicity amplitudes $A_{1/2}(Q^2)$ and $S_{1/2}(Q^2)$ for the electroproduction of $N^*(1535)$ resonance using lattice results for the N^* distribution amplitudes [96] compared to the available experimental data. The points at $Q^2 < 5.0$ GeV^2 are from the CLAS data analysis [191]. The points at $Q^2 > 5.0$ GeV^2 are the Hall C data [97], obtained under the assumption $A_{1/2} >> S_{1/2}$. The curves are obtained using central values of lattice parameters and the shaded areas show the corresponding uncertainty.

bilocal contributions to the operator product expansion.

In order to match the expected accuracy of the next generation of lattice results, the LCSR calculations of baryon form factors will have to be advanced to include NLO radiative corrections, as it has become standard for meson decays. For the first effort in this direction, see [98]. In addition, it is necesary to develop a technique for the resummation of "kinematic" corrections to the sum rules that are due to nonvanishing masses of the resonances. The corresponding corrections to the total cross section of the deep-inelastic scattering are known as Wandzura-Wilczek corrections and can be resummed to all orders in terms of the Nachtmann variable; we will be looking for a generalization of this method to non-forward kinematics which is also important in a broader context. With these improvements, we expect that the LCSR approach can be used to constrain light-cone DAs of the nucleon and its resonances from the comparison with the electroproduction data. These contraints can then be compared with the LQCD calculations.

V. GPD AND LCSR REPRESENTATIONS OF RESONANCE FORM FACTORS

One of the primary goals of the JLab upgrade, and CLAS12 in particular, is to characterize the wave functions of the nucleon and its excitation in terms of the current quark and gluon fields. In principle, these wave functions can be constrained experimentally through measurements of exclusive reactions over large ranges of x and t. Baryon elastic and transition form factors can be written as overlap integrals of the light-cone wave functions, and make an important contribution to this program. There are several approaches to encoding these overlap integrals in terms of the partonic degrees of freedom, i.e. x and t, which connect them to the experimental data. Two examples we discuss here are generalized parton distributions (GPD) and the light cone sum rule (LCSR), which were discussed in the previous contribution to these proceedings [99]. In particular, we focus on how they specifically relate to the measured form factors. These overlap integrals are the connecting points between theory and experiment. At this time the theoretical approach which most directly links QCD to these observables appears to be lattice QCD (LQCD). The goals of LQCD are to calculate the GPDs or DAs which can be fed into the basic relationships which predict the experimental results.

GPDs and Resonance Form Factors.

The extraction of GPDs from experiments on exclusive reactions at high momentum transfer, such as deeply virtual Compton scattering (DVCS) and deeply virtual meson production, is one of the primary goals of the CLAS12 upgrade. Since elastic and baryon transition form factors are the first moments of the GPDs, they provide important constraints and thus provide a vital contribution to the overall exclusive reaction program. The relationship of models of GPDs and elastic form factors have been treated in detail, for example in Ref. [100].

The N $\rightarrow$ $\Delta(1232)$:

The relationships between GPDs and resonance form factors was worked out and treated several years ago in Refs. [101] [102]. The current structure of the transition

$$\Gamma_{\nu\mu} = G_M^*(q^2)K_{\nu\mu}^M(q^2) + G_E^*(q^2)K_{\nu\mu}^E(q^2) + G_C^*(q^2)K_{\nu\mu}^C(q^2)$$

leads to the following GPD relation:

$$\frac{P^+}{2\pi}\int dy^- e^{ix\bar{P}^+y^-}\,\langle\Delta(p')|\,\bar{\psi}_\Delta\,(-y/2)\,\gamma_\nu n^\nu\tau_3\psi\,(y/2)\,|N(p)\rangle\Big|_{y^+=\vec{y}_\perp=0} = \bar{u}^\beta_\Delta(p')\left\{H_M(q^2)K^M_{\beta\mu}(q^2)+H_E(q^2)K^E_{\beta\mu}(q^2)+H_C(q^2)K^C_{\beta\mu}(q^2)\right\}n^\mu u_p(p) \quad (4)$$

In eq. (4) above, $u^\beta_\Delta(p')$ is a Rarita-Schwinger spinor for the Δ, $K^{M,E,C}_{\beta\mu}$ are the covariants defined in [103], n^μ is a light-cone vector normalized such that $n^2=0$ and $n^\mu P_\mu = 1$. The relationship between the form factors and the GPDs is then

$$2G^*_M(t)=\int dx H_M(t,x,\xi),\quad 2G^*_E(t)=\int dx H_E(t,x,\xi)\ \text{ and }\ 2G^*_C(t)=\int dx H_C(t,x,\xi).$$

The first practical application of GPDs to resonances were reported in [104] for the $N\to\Delta$ transition. It was shown that the anomalously rapid falloff of the G^*_M can be directly related to the unexpectedly rapid falloff of the elastic helicity flip F_2, which had been recently discovered, by constraining the $N\to\Delta$ GPD by the isovector part of the elastic scattering form factors. Figure 10 shows a more recent [105] fit to G^*_M, which was obtained from GPDs constrained from elastic scattering using a Regge like parameterization. The Fourier transform of the GPD gives the distribution of the impact parameter [106] in the transverse plane vs. the longitudinal momentum fraction, i.e. $H_M(\vec{b}_\perp,x)$, also shown in Fig. 10 .

$$H_M(x,\vec{b}_\perp)=\int\frac{d^2(\vec{q}_\perp)}{2\pi^2}e^{i(\vec{b}_\perp\cdot\vec{q}_\perp)}H_M(-\vec{q}^2_\perp,x,0).$$

The application of the GPD formalism to nucleon excitation is most readily seen in the $J=1/2\to1/2$ transitions such as the $N\to P_{11}(1440)$ or the $S_{11}(1535)$.

The $N\to P_{11}(1440)$:

Since the $N\to P_{11}(1440)$ is a $1/2^+\to1/2^+$ transition, its current structure is similar to elastic scattering, i.e.

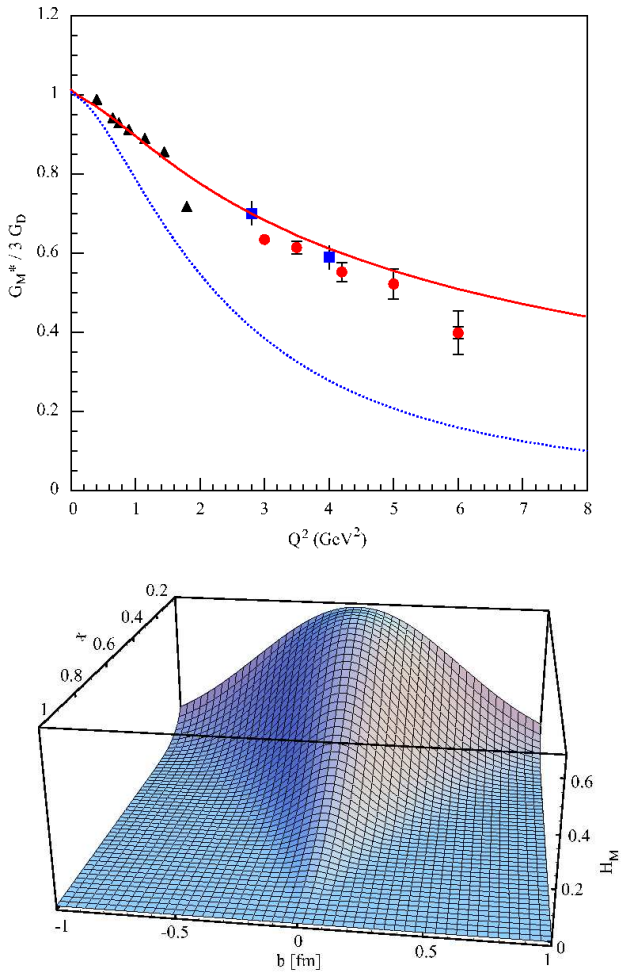

FIG. 10: Top: The red curve represents the form factor G_M^* obtained by [105] using a Regge like parameterization of the elastic isovector form factor applied to the $N \to \Delta$ transition. Bottom: The distribution of the transverse impact parameter $\vec{b}_\perp$ and longitudinal imomentum.

$$\Gamma^\mu_{P11} = \frac{F_1^{P11}(q^2)}{M_N^2}\left(q^2\gamma^\mu - \not{q}q^\mu\right) + \frac{F_2^{P11}(q^2)}{2M_N} i\sigma^{\mu\nu}q_\nu$$

which immediately leads to a GPD structure and related form factors exactly as in elastic scattering:

$$\frac{P^+}{2\pi}\int dy^- e^{ix\bar{P}^+y^-}\left\langle P_{11}(p')\right|\bar{\psi}_{P11}\left(-y/2\right)\gamma^\nu n_\nu \psi\left(y/2\right)\left|N(p)\right\rangle\Big|_{y^+=\vec{y}_\perp=0} =$$
$$H_{P11}\bar{u}(p')\frac{\left(q^2\gamma^\mu - \not{q}q^\mu\right)n_\mu}{M_N^2}u(p) + E_{P11}\bar{u}(p')i\sigma^{\mu\nu}\frac{n_\mu q_\nu}{2M_N}u(p) \qquad (5)$$

$$F^q_{1P_{11}}(t) = \int H^q_{P_{11}}(x,\xi,t)dx \quad F^q_{2P_{11}}(t) = \int E^q_{P_{11}}(x,\xi,t)dx$$

The N $\rightarrow$ S_{11}(1535): The $S_{11}(1535)$ has $J^\pi = 1/2^-$ and is the chiral negative parity partner of the nucleon. The current structure has an extra γ_5 and can be written

$$\Gamma^\mu_{S11} = \frac{F_1^{S11}(q^2)}{M_N^2}\left(q^2\gamma^\mu - \not{q}q^\mu\right)\gamma_5 + \frac{F_2^{S11}(q^2)}{2M_N} i\sigma^{\mu\nu}q_\nu\gamma_5$$

which leads to

$$\frac{P^+}{2\pi}\int dy^- e^{ixP^+y^-}\left\langle S_{11}(p')\right|\bar{\psi}_{S11}\left(-y/2\right)\gamma^\nu n_\nu\psi\left(y/2\right)\left|N(p)\right\rangle\Big|_{y^+=\vec{y}_\perp=0} =$$
$$H_{S11}\bar{u}(p')\frac{(q^2\gamma^\mu - \not{q}q^\mu)\,n_\mu}{M_N^2}\gamma_5 u(p) + E_{S11}\bar{u}(p')i\sigma^{\mu\nu}\gamma_5\frac{q^\nu n_\mu}{2M_N}u(p) \qquad (6)$$

with

$$F^q_{1S_{11}}(t) = \int H^q_{S_{11}}(x,\xi,t)dx \quad F^q_{2S_{11}}(t) = \int E^q_{S_{11}}(x,\xi,t)dx$$

The N $\rightarrow$ Λ, Σ: Hard exclusive processes with strangeness production was treated in Refs. [101] and [102], in which effects related to $SU(3)$ flavor symmetry-breaking are discussed. The GPDs correspond to the process where a non-strange quark is taken out of the initial nucleon at the space-time point $y/2$, and then a strange quark is put back exciting a hyperon at the space-time point $y/2$. Following Ref. [101] the strangeness changing distributions for $N \rightarrow \Sigma, \Lambda$ transitions:

$$\frac{P^+}{2\pi}\int dy^- e^{ixP^+y^-}\left\langle Y(p')\right|\bar{\psi}\left(-y/2\right)\bar{a}_s\left(-y/2\right)\gamma^\nu n_\nu a_q\left(y/2\right)\psi\left(y/2\right)\left|N(p)\right\rangle\Big|_{y^+=\vec{y}_\perp=0} =$$
$$H_{N\rightarrow Y}\bar{u}(p')\frac{(q^2\gamma^\mu - \not{q}q^\mu)\,n_\mu}{M_N^2}\gamma_5 u(p) + E_{N\rightarrow Y}\bar{u}(p')i\sigma^{\mu\nu}\gamma_5\frac{q^\nu n_\mu}{2M_N}u(p) \qquad (7)$$

where $\bar{a}_s$ is the creation operator of a strange quark and $\bar{a}_q$ the annihilation operator of a non-strange quark, u or d, at $-y/2$ and $y/2$, respectively.

Light Cone Sum Rules (LCSR).

The Light-Cone Sum Rule (LCSR) approach allows one to calculate form factors (and, potentially, also GPDs) using much more limited information compared to the full nonperturbative wave functions, albeit with some assumptions. The groundwork of the method of LCSRs was laid in [107]. Following the work [83, 84] devoted to electromagnetic nucleon form factors the $N \to \Delta$ transitions were considered in [93] and the $N \to S_{11}$ transitions in [108]. LCSRs have also been applied to threshold pion electroproduction [94, 95].

For example, in order to calculate the transition amplitude

$$\left\langle N_{S11}\left(P'\right)\left|j_{\mu}^{em}\right|N\left(P\right)\right\rangle = N_{S11}\left(P'\right)\left(F_1^{S11}(q^2)\frac{(q^2\gamma_\mu - \not{q}q_\mu)}{M_N^2}F_2^{S11}(q^2)i\sigma_{\mu\nu}\frac{q^\nu}{2M_N}\right)\gamma_5 N\left(P\right) \tag{8}$$

one considers the correlation function

$$\int dx\, e^{-iqx}\langle S11(P')|T\{\eta(0)j_\mu^{\rm em}(x)\}|0\rangle$$

in which η is a suitable operator with nucleon quantum numbers. A popular choice is, for example

$$\eta(0) = \epsilon^{ijk}(u_i C\gamma_\mu u_j)(0)\gamma_5\gamma^\mu d_k(0) \tag{9}$$

where $u_{i,j}(0)$ and $d_k(0)$ are u-quark and d-quark field operators, $i,j,k = 1,\ldots,3$ is the color index; C is the charge conjugation matrix. The electromagnetic current is

$$j_\mu^{\rm em}(x) = e_u\bar{u}(x)\gamma_\mu u(x) + e_d\bar{d}(x)\gamma_\mu d(x) + e_s\bar{s}(x)\gamma_\mu s(x) \tag{10}$$

Making use of the duality of QCD quark-gluon and hadronic degrees of freedom through dispersion relations one can write a representation for the form factors appearing in (8) in terms of the distribution amplitudes (DAs) of the S_{11} resonance. These DAs correspond to the momentum fraction distributions of the three quarks in the S_{11} at small transverse separations. Unlike the S_{11} wave functions themselves, the DAs can be accessed through lattice calculations.

The leading twist-3 nucleon (proton) DA can be defined as a matrix element of the nonlocal light-ray operator that involves quark fields of given helicity $q^{\uparrow(\downarrow)} = (1/2)(1 \pm \gamma_5)q$

$$\langle 0|\epsilon^{ijk}\Big(u_i^{\uparrow}(a_1n)C\not{n}u_j^{\downarrow}(a_2n)\Big)\not{n}d_k^{\uparrow}(a_3n)|N(P)\rangle = \\ = -\frac{1}{2}f_N\, pn\, \not{n}\, u_N^{\uparrow}(P)\int[dx]\, e^{-ipn\sum x_i a_i}\,\varphi_N(x_i)\,. \tag{11}$$

Here P_μ, $P^2 = m_N^2$, is the proton momentum, $u_N(P)$ is the usual Dirac spinor in relativistic normalization, n_μ an arbitrary light-like vector with $n^2 = 0$, as defined above, and C the charge-conjugation matrix. The variables x_1, x_2, x_3 have the meaning of the momentum fractions carried by the three valence quarks and the integration measure is defined as $\int[dx] = \int_0^1 dx_1 dx_2 dx_3 \delta(\sum x_i - 1)$. The Wilson lines that ensure gauge invariance are inserted between the quarks; they are not shown for brevity.

The definition in (11) is equivalent to the following form of the valence proton state

$$|p,\uparrow\rangle = f_N \int \frac{[dx]\,\varphi_N(x_i)}{2\sqrt{24x_1x_2x_3}}\left\{|u^{\uparrow}(x_1)u^{\downarrow}(x_2)d^{\uparrow}(x_3)\rangle - |u^{\uparrow}(x_1)d^{\downarrow}(x_2)u^{\uparrow}(x_3)\rangle\right\}, \tag{12}$$

where the arrows indicate the helicities and the standard relativistic normalization for the states and Dirac spinors is implied.

The nonlocal operator appearing on the l.h.s. of (11) does not have a definite parity. Thus the same operator couples also to $N^*(1535)$ and one can define the corresponding leading-twist DA as

$$\langle 0|\epsilon^{ijk}\Big(u_i^{\uparrow}(a_1n)C\not{n}u_j^{\downarrow}(a_2n)\Big)\not{n}d_k^{\uparrow}(a_3n)|N_{S11}(P)\rangle = \\ = \frac{1}{2}f_{N^*}\, pn\, \not{n}\, u_{S11}^{\uparrow}(P)\int[dx]\, e^{-ipn\sum x_i a_i}\,\varphi_{S11}(x_i) \tag{13}$$

where, of course, $P^2 = m_{N^*}^2$. The normalization constants f_N, f_{N^*} are defined such that the DAs are normalized to unit integral:

$$\int[dx]\;\varphi(x_i) = 1\,. \tag{14}$$

As an example of the results of the LCSR calculation of the helicity amplitides A_{11} and S_{11} obtained by [96, 108] using the lattice QCD estimates of the relevant distribution amplitudes

[92], is shown in Figs 1 and 2 of the contribution of V. Braun [99] to these proceedings.

To close the circle, one can relate the LCSR matrix element to the GPDs:

$$\left\langle N_{S11}\left(P'\right)\left|j_{\mu}^{em}\right|N\left(P\right)\right\rangle \sim \int dx H_{S11}\bar{u}(p')\frac{(q^2\gamma^{\mu}-\not{q}q^{\mu})}{M_N^2}\gamma_5 u(p)+\int dx E_{S11}\bar{u}(p')i\sigma^{\mu}\gamma_5\frac{q^{\nu}}{2M_N}u(p) \tag{15}$$

VI. CONSTITUENT QUARK MODELS

The study of hadron properties can be performed within a microscopic approach based on quark degrees of freedom and their interactions. The widely accepted framework is provided by Quantum ChromoDynamics (QCD), which is of course fully relativistic, however it is usable only in particular conditions, mainly at high momentum transfer. There are now many important results in the Lattice QCD (LQCD) but the present computer capabilities do not yet allow to extract all the hadron properties in a systematic way. In the meanwhile, one can rely on models, eventually based on QCD or LQCD. An important class of such models is provided by Constituent Quark Models (CQM), in which quarks are considered as effective internal degrees of freedom and can acquire a mass and even, in certain approaches, a finite size. There are many versions of CQM, which differ according to the chosen quark dynamics: one-gluon exchange and a three-body force [109, 110, 111], algebraic [112], hypercentral (hCQM) [113], Goldstone Boson Exchange (GBE) [114],instanton [115]. In most cases they have been applied to the description of many hadron properties (spectrum, elastic form factors, transition form factors,...) and have also been relativized.

The construction of a Relativistic Constituent Quark Model (RCQM) means a) the use of a relativistic kinetic energy for the quarks; b) the application of Lorentz boosts in order to describe baryons in motion; c) the formulation of quark dynamics within a relativistic hamiltonian using one of the forms introduced by Dirac: front, instant or point form which provide different realizations of the Poincaré group. Of course c) implies also both a) and b). An alternative way of building a relativistic baryon description is given by a Bethe-Salpeter approach (BS) [14, 115]. As far as the spectrum is concerned, a) is often the only relativistic aspect which is considered, however, in electron scattering the recoil of the struck nucleon becomes relativistic as the momentum transfer increases. However, when baryon resonances

are excited, such effects may be softened because of the higher mass of the recoiling resonance [116].

There are now many results obtained with relativistic Constituent Quark Models (RCQM). The relativized h.o. with light front has been applied to the calculation of the elastic nucleon form factors and of $\gamma_v NN^*$ helicity amplitudes [5, 6, 7, 8, 111, 117]. A good description of the nucleon elastic form factors is obtained both in the GBE model in the point and front forms [118, 119] and in the instanton BS approach [115]. The hCQM has been used for a systematic prediction of the helicity amplitudes [9] (although in its non relativistic version) and of the elastic form factors in a fully relativistic formulation using the point form [120]. Comparing these predictions with the helicity amplitudes data [9], one observes a systematic lack of strength, which, according to a wide consensus, is ascribed to the missing $q\bar{q}$ pairs in the outer region [121]. For medium Q^2 the behaviour is fairly well reproduced, although some discrepancies arise, probably because relativity is not taken into account completely [116]. On the other hand, the prediction for the elastic form factors is close to the data, but a very good fit is obtained by introducing quark form factors (Fig. 11).

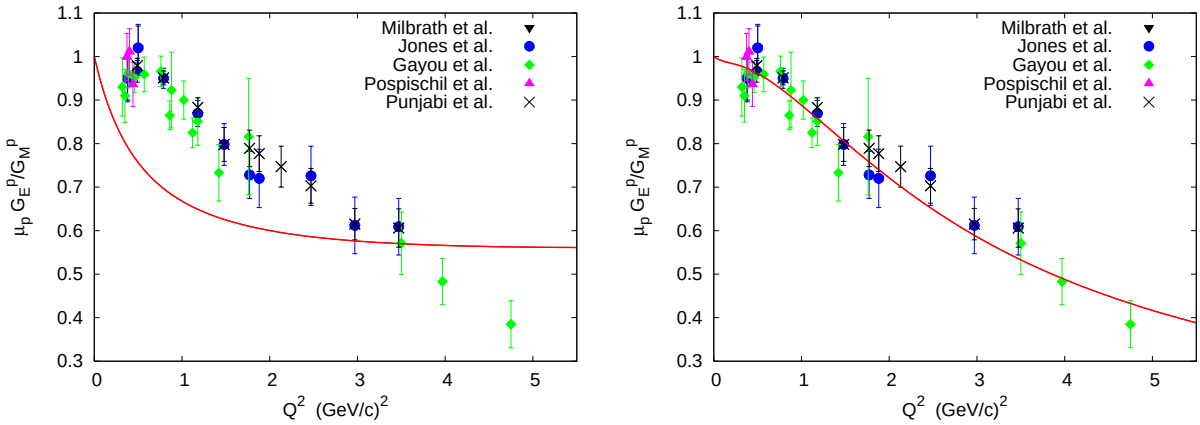

FIG. 11: The ratio $G_E^p/\mu_p G_M^p$ calculated with the hCQM [120], without (left) and with (right) constituent quark form factors. Data are in ref. [120].

The two aspects just mentioned, the $q\bar{q}$ pair effects and the quark form factors presumably will play a key role in the description of the baryon excitation in the Q^2 range accessible with 12 GeV electrons. This is certainly a transition region between the phase where the CQ with mass and size are the dominant degrees of freedom and the range where the asymptotic behaviour dominated by current quarks starts to be effective. The presence of $q\bar{q}$ (or meson

cloud) effects points towards the unquenching of the quark models [121]. This problem has been addressed for the meson sector within the flux tube model [122] but recently also the baryon sector has been studied [123]. With the availability of unquenched CQM, it will be possible to describe the microscopic mechanisms leading to the excitation of resonances and the production of mesons. Therefore both the electromagnetic and strong decay of the resonances will be described in a consistent way. The description of the spectrum will be also more realistic. In fact, in all the presently used CQM, the energies of the baryon resonanances are sharply defined, while in an unquenched approach the excited states acquire a non zero width thanks to the coupling with the continuum.

The meson cloud effects are certainly relevant in the low Q^2 region [124]. A calculation with a dynamical model [125] shows that actually the contribution of the pion cloud to the helicity amplitudes decreases with increasing Q^2 and seems to partially compensate the lack of strength of the CQM calculations. However, with increasing momentum transfer the excitation of resonances will also allow testing of the short distance behaviour of the $q\bar{q}$ production mechanism and, in particular, of the meson production.

The availability of high-intensity electron beams at 12 GeV will also allow the probing at high Q^2 of baryons that have a more complicated structure than a simple three quark configuration. If multiquark configurations, such as $qqqq\bar{q}$, can mix with the conventional three-quark components of a baryon, they may have a different Q^2-dependence compared with the qqq component [11, 126]. The phenomenological quark form factors which have been introduced up to now contain and mix contributions from both the structure of the effective (consituent) quarks and from the dynamics not explicitly included in CQM, such as the $q\bar{q}$ pair creation or meson production effects. By unquenching the CQM, it will be possible to disentangle the quark form factors and test the onset of the transition to the asymptotic QCD current quarks.

In absence of a consistently unquenched approach, one can use the CQM in order to provide constraints on the parameters describing the leading order baryon-photon and baryon-meson vertices by considering explicit quark-photon and quark meson couplings. In exclusive meson production channels, an economic way to include a complete set of intermediate baryon resonances is the introduction of effective Lagrangians for the constituent-quark-meson couplings. One can then explicitly construct transition operators and by studying their Q^2 evolution one can establish relations between the internal quark motions and EM

and strong form factors in exclusive meson electroproduction reactions. Various quark model approaches for the reaction process can be tested and compared with systematic experimental measurements.

Quark-hadron duality has been one of the most striking phenomena observed in electron-proton inclusive scattering, where the low-energy exclusive resonance excitations are related to the high-energy inclusive scaling behaviour through a local average over the resonance structure functions. Recent experimental data from JLab have tested this empirical phenomenon to high precision and initiated renewed interest in this field. In particular, the idea of quark-hadron duality has been used in a recent analysis [127] which allowed to identify objects inside the proton having a finite constituent size and non-zero form factors. The role of quark-hadron duality has been investigated also in exclusive meson photoproduction, where a restricted locality of quark-hadron duality was shown to be important [128] and related to deviations from the pQCD counting rules above the resonance region. In the quark model framework, the resonance phenomena are dual to the quark motion correlations and the study of vector meson photo- and electroproduction from low to high Q^2 is expected to allow an interesting test of this phenomenon, and shed light on the transition between the perturbative and strong interaction regimes of QCD.

Therefore, the excitation at high Q^2 of resonances may provide new information concerning the fundamental underlying QCD mechanisms responsible for the baryon structure and quark confinement.

To conclude, the NRCQM has provided a consistent framework for the description of a large number of hadron properties. However, in order to be applcable to the high Q^2 regime, the CQM not only has to be formulated in a consistent relativized framework, according to the methods mentioned above, but it should also include another fundamental relativistic requirement, that of the possibility of the creation of quark-antiquark pairs.

VII. STATUS OF JLAB DATA ANALYSIS

N^* studies in meson electroproduction with CLAS

The comprehensive experimental data set obtained with the CLAS detector on single pseudoscalar meson electroproduction, e.g. $p\pi^0$, $n\pi^+$, $p\eta$, and $K\Lambda$ [81, 129, 130, 131, 132,

133, 134, 135, 136, 137, 138, 139, 140, 141] and double charged pion electroproduction [142, 143, 144, 145] opens up new opportunities for studies of the $\gamma_v NN^*$ transition helicity amplitudes (i.e. the N^* electrocoupling parameters) [146, 147, 148]. The CLAS data for the first time provided information on many observables in these exclusive channels, including fully integrated cross sections and a variety of 1-fold differential cross sections complemented by single and double polarization asymmetries in a range of Q^2 from 0.2 to 4.5 GeV^2. This comprehensive information makes it possible to utilize well established constraints from dispersion relations and to develop phenomenological approaches in order to determine the Q^2-evolution of the N^* electrocoupling parameters by fitting them to all available observables combined. Several phenomenological analyses of the experimental data on single (1π) and charged double pion (2π) electroproduction have already been carried out within the CLAS Collaboration [170, 171, 172, 173, 174, 175, 177, 178]. They allowed us to determine transition helicity amplitudes and the corresponding transition form factors for a variety of low lying states: $P_{33}(1232)$, $P_{11}(1440)$, $D_{13}(1520)$, $S_{11}(1535)$ at photon virtualities from 0.2 to 4.5 GeV^2. Typical examples for resonance electrocoupling parameters are shown in Fig. 16. The 2π data enhance substantially our capabilities for the studies of N^* with masses above 1.6 GeV. Many of these resonances decay predominantly to N$\pi\pi$ final states. The analysis of 2π data at W $>$ 1.6 GeV allowed us for the first time to map out the Q^2 evolution of electrocoupling parameters for resonances with masses above 1.6 GeV that preferably decay by 2π emission: $S_{31}(1620)$, $D_{33}(1700)$ and $P_{13}(1720)$ [175, 176]. In analysis of the 2π electro production data [142] we observed a signal from a $3/2^+(1720)$ candidate state whose quantum numbers and hadronic decays parameters are determined from the fit to the measured data.

There are up to three transition helicity amplitudes $A_{1/2}(Q^2)$, $A_{3/2}(Q^2)$, and $S_{1/2}(Q^2)$, that fully describe the excitation of a resonance by virtual photons. Resonance excitations may also be described in terms of $F_1^*(Q^2)$, $F_2^*(Q^2)$ or $G_E^*(Q^2)$, $G_M^*(Q^2)$ transition form factors (for states with spin $> 1/2$ we also have a third form factor in both representations), that are used in the electromagnetic $N \to N^*$ transition current. They play a similar role as the elastic form factors. The descriptions of resonance excitations by transition form factors or transition helicity amplitudes are equivalent and can be uniquely expressed in terms of each other [189]. They can be determined either by fitting resonance parts of production amplitudes within the framework of a Breit-Wigner ansatz [179] or by applying various

multi-channel resonance parameterizations [184].

Full production amplitudes in all meson electroproduction channels represent a superposition of resonant contributions and complicated non-resonant processes. In order to determine the N^* electrocoupling parameters a reliable separation of resonant and non-resonant parts contributing to the meson electroproduction amplitudes is needed. This is one of the most challenging problems for the extraction of N^* electrocoupling parameters. The amplitudes of effective meson-baryon interactions in exclusive electroproduction reactions cannot be expanded in a small parameter over the entire resonance region. It is impossible to select contributing diagrams through a perturbative expansion. So far, no approach has been developed that is based on a fundamental theory and that would allow either a description of an effective meson-baryon Lagrangian or a selection of the contributing meson-baryon mechanisms from first principles. We therefore have to rely on fits to the comprehensive experimental data of various meson electroproduction channels from CLAS to develop reaction models that contain the relevant mechanisms. This approach allows us to determine all the essential contributing mechanisms based on their manifestations in the kinematic dependencies of measured observables.

Nucleon resonances have various decay modes and hence manifest themselves in different meson electroproduction channels. Contributions of non-resonant amplitudes are substantially different in the different meson electroproduction channels [148, 185]. On the other hand, the N^* electrocoupling parameters remain the same in all meson electroproduction channels. They are fully determined by the $\gamma_v NN^*$ vertices and independent from the hadronic decay of the resonance. The successful description of a large body of observables in various exclusive channels with a common set of N^* electrocoupling parameters gives evidence that the $\gamma_v NN^*$ helicity amplitudes can be reliably determined from different hadronic final states. In the future, this analysis will be carried out in a complete coupled channel approach which is currently being developed at EBAC [186, 187, 188].

1π and 2π electroproduction are the two dominating exclusive channels in the resonance region. The 1π exclusive channel is mostly sensitive to N^*'s with masses lower than 1.65 GeV. Many resonances of heavier masses decay predominantly by two pion emission. Thus the 2π exclusive channel offers better opportunities to study the electrocoupling parameters of these high-lying states. The final states in 1π and 2π channels have considerable hadronic interactions. The cross section for the $\pi N \to \pi\pi N$ reaction is the second largest of all of

the exclusive channels for πN interactions. Therefore, for N^* studies both in single and double pion electroproduction, information on the mechanisms contributing to each of these channels is needed in order to take properly into account the impact from coupled-channel effects on the exclusive channel cross sections. The knowledge of single and double pion electroproduction mechanisms becomes even more important for N^* studies in channels with smaller cross sections such as $p\eta$ or $K\Lambda$ and $K\Sigma$ production, as they can be significantly affected in leading order by coupled-channel effects produced by their hadronic interactions with the dominant single and double pion electroproduction channels. Comprehensive studies of single and double pion electroproduction are of key importance for the entire baryon resonance research program.

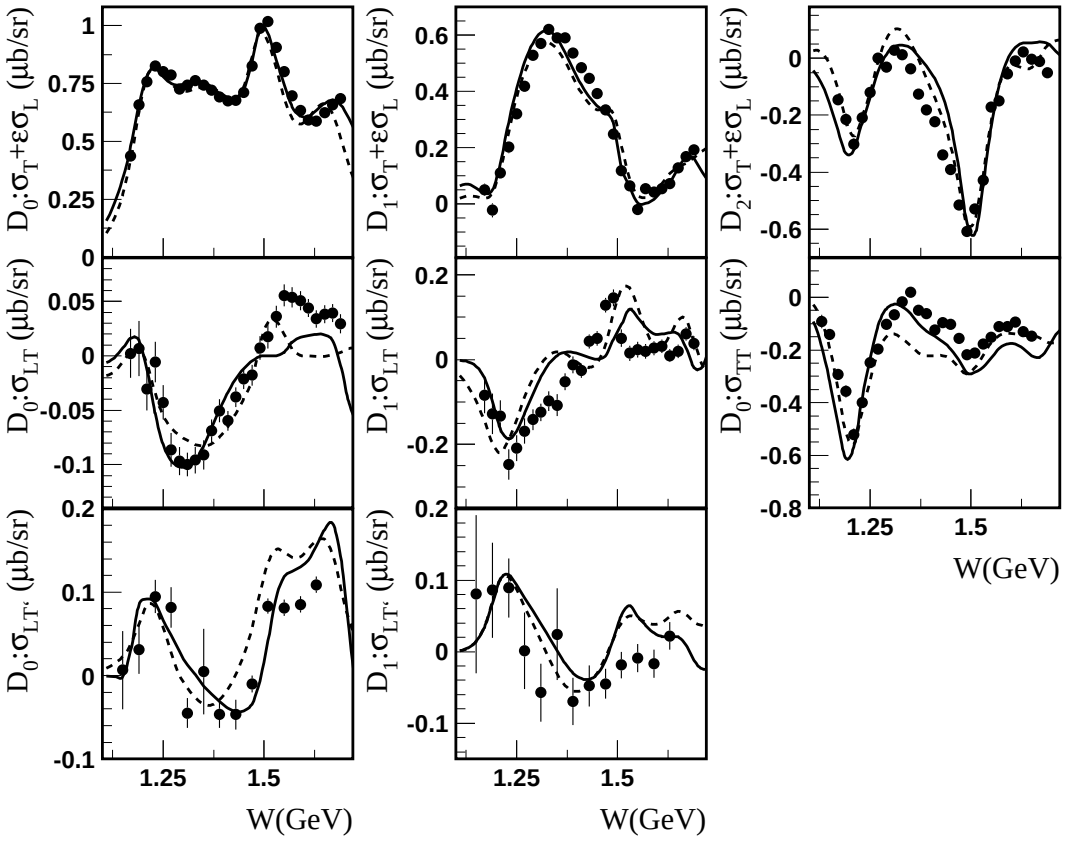

FIG. 12: The results for the Legendre moments of the $\vec{e}p \to en\pi^+$ structure functions in comparison with experimental data [136] for $Q^2 = 2.44$ GeV^2. The solid (dashed) curves correspond to the analyses made using DR (UIM) approach.

Analysis approaches for the single meson electroproduction data

Over the past 40 years, our knowledge of electromagnetic excitations of nucleon resonances

was mainly based on single pion photo- and electroproduction. These reactions have been the subject of extensive theoretical studies based on dispersion relations and isobar models. The dispersion relation (DR) approach has been developed on the basis of the classical works [150, 151] and played an extremely important role in the extraction of the resonance contributions from experimental data. Dispersion relations provide stringent constraints on the real part of the reaction amplitudes that contain the most significant part of the non-resonant contributions. Starting in the late 1990's the Unitary Isobar Model [152] (also known as MAID), became widely used for the description of single-pion photo- and electroproduction data. Later this approach has been modified [170] by incorporating Regge poles to describe the high energy regime. This extension of the isobar model enables a good description of all photo-production multipole amplitudes with angular momenta $l \leq 3$ up to an invariant mass $W = 2$ GeV using a unified Breit-Wigner parametrization of the resonance contributions in the form as proposed by Walker [149]. Dispersion relations and the Unitary Isobar Model (UIM) [170] have been successfully used for the analysis [171, 172, 173] of the CLAS [81, 129, 130, 131, 133, 136] and the world data to extract resonance electrocouplings from the data on cross sections and longitudinally polarized electron beam asymmetries for the reactions $p(\vec{e}, e'p)\pi^0$ and $p(\vec{e}, e'n)\pi^+$ in the first and second resonance region. The quality of these results is best characterized by the following χ^2 values: $\chi^2 < 1.6$ at $Q^2 = 0.4$ and 0.65 GeV^2 and $\chi^2 < 2.1$ at $1.7 < Q^2 < 4.5$ GeV^2. In the analyses [170, 171, 172, 173], the Q^2 evolution of the electrocoupling amplitudes for the lower-lying resonances with $W < 1.6$ GeV have been established for Q^2s up to 4.5 GeV^2. The comparison of two conceptually different approaches, DR and UIM, allows us to conclude that the model-dependence of the obtained results is relatively small.

The background in both approaches, DR and UIM, contains Born terms corresponding to s- and u-channel nucleon exchanges and the t-channel pion contribution, and thus depends on the proton, neutron, and pion form factors. The background of the UIM contains also the ρ and ω t-channel exchanges, and thus contributions of the form factors $G_{\rho(\omega)\to\pi\gamma}(Q^2)$. The proton magnetic and electric form factors as well as the neutron magnetic form factor are known from the existing experimental data, for Q^2 up to 32, 6, and 10 GeV^2, respectively [153, 154, 155, 156, 157, 158, 159, 160, 161, 162]. This information on the proton and neutron elastic form factors combined with the parametrization of the proton electric form factor from polarization experiments [163] can be readily used for the analysis of the pion

electroproduction data up to quite large values of Q^2. The neutron electric form factor, $G_{E_n}(Q^2)$, is measured up to $Q^2 = 1.45$ GeV^2 [72]. A parametrization of all existing data on $G_{E_n}(Q^2)$ [72] can be used to extrapolate $G_{E_n}(Q^2)$ to higher four momentum transfers. The pion form factor $G_\pi(Q^2)$ has been studied for Q^2 values from 0.4 to 9.8 GeV^2 at CEA/Cornell [164, 165] and more recently at JLab [166, 167]. All these measurements show that the Q^2 dependence of $G_\pi(Q^2)$ can be described by a simple monopole form $1/(1+\frac{Q^2}{0.46\ \mathrm{GeV}^2})$ [164, 165] or $1/(1+\frac{Q^2}{0.54\ \mathrm{GeV}^2})$ [166, 167], respectively. There are no measurements on the $G_{\rho(\omega)\to\pi\gamma}(Q^2)$ form factors. However, investigations, one based on QCD sum rules [168] and another one on a quark model [169], predict that the Q^2 dependence of these form factors follows closely the dipole form. Therefore our corresponding background estimations proceed from the assumption that $G_{\rho(\omega)\to\pi\gamma}(Q^2) \sim 1/(1+\frac{Q^2}{0.71\ \mathrm{GeV}^2})^2$.

In figure 12 we present as an example, the description of $\vec{e}p \to en\pi^+$ data [136] for one specific Q^2 value. The results are shown in terms of the Legendre moments of structure functions. This allows us to compare the analysis results with experimental data for all energies and angles.

Meson-baryon model approach JM for the 2π electroproduction analysis

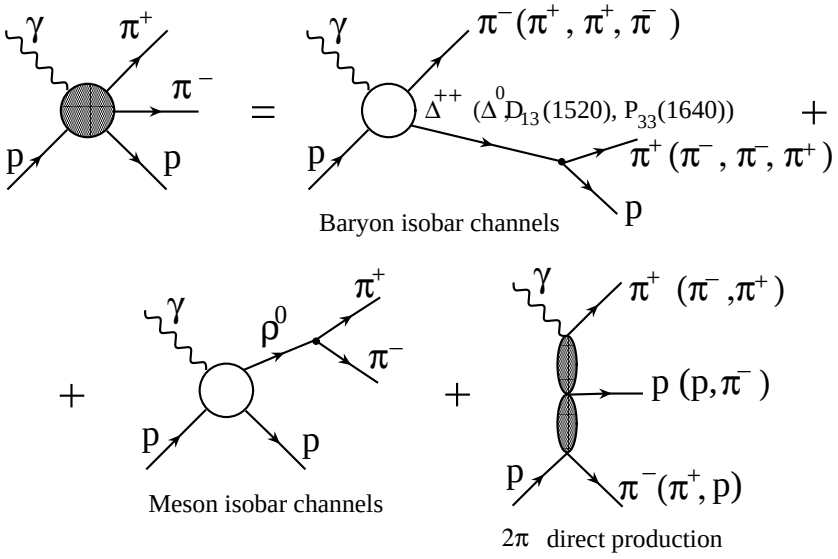

FIG. 13: The mechanisms of the JM model.

A comprehensive data set on 2π single-differential and fully-integrated electroproduction cross sections measured with CLAS has enabled us to establish the presence and strengths of the essential $p\pi^+\pi^-$ electroproduction mechanisms. This was achieved within the framework of a phenomenological model that has been developed over the past several years by the Jefferson Laboratory - Moscow State University collaboration (JM) [172, 174, 175, 177, 178, 180, 181, 182, 183] for the analysis of 2π photo- and electroproduction data. In this approach the resonant part of the amplitudes is isolated and the Q^2 evolution of the individual electrocoupling parameters of the contributing nucleon resonances are determined from a simultaneous fit to all measured observables.

The mechanisms of 2π electroproduction incorporated into the JM model are illustrated in Fig. 13. The full amplitudes are described by superposition of the $\pi^-\Delta^{++}$, $\pi^+\Delta^0$, ρp, $\pi^+D^0_{13}(1520)$, $\pi^+F^0_{15}(1685)$, and $\pi^-P^{++}_{33}(1600)$ isobar channels and the direct 2π production mechanisms, where the $\pi^+\pi^-p$ final state is directly created without the formation of unstable hadrons in the intermediate states. Nucleon resonances contribute to the baryon $\pi\Delta$ and meson ρp isobar channels. The respective resonant amplitudes are evaluated in a Breit-Wigner ansatz, as described in [180]. We included all well-established resonance states with hadronic decays to $N\pi\pi$ and an additional $3/2^+(1720)$ candidate state. Evidence for this candidate state was found in the analysis of the CLAS 2π electroproduction data [142].

The $\pi\Delta$ isobar channels are strongest contributors to the 2π electroproduction up to an invariant mass of $W \sim 2.0$ GeV. They have been clearly identified in the π^+p and π^-p 1-fold differential mass distribution cross sections. The non-resonant $\pi\Delta$ amplitudes are calculated from the well established Reggeized Born terms [178, 179, 180]. The initial and final state interactions are described by an effective absorptive-approximation [180]. An additional contact term has been introduced in [174, 175, 178] to account phenomenologically for all remaining possible production mechanisms through the $\pi\Delta$ intermediate state channels, as well as for remaining FSI effects. The parametrization for these amplitudes can be found in [178].

The ρp isobar channel becomes visible in the data at $W > 1.65$ GeV with significant resonant contributions for $W < 2.0$ GeV. Here the non-resonant amplitudes are estimated by a diffractive ansatz, that has been modified in order to reproduce experimental data in the near and sub-threshold regions [183].

The contributions from $\pi^+D^0_{13}(1520)$, $\pi^+F^0_{15}(1685)$, $\pi^-P^{++}_{33}(1640)$ isobar channels are

seen in $\pi^- p$ and $\pi^+ p$ mass distributions at $W > 1.65$ GeV. The $\pi^+ D^0_{13}(1520)$ amplitudes are derived from the Born terms of the $\pi\Delta$ isobar channels by implementing an additional γ_5-matrix that accounts for the opposite parity of the $D_{13}(1520)$ with respect to the Δ. The amplitudes of $\pi^+ F^0_{15}(1685)$ and $\pi^- P^{++}_{33}(1640)$ isobar channels are parametrized as Lorentz invariant contractions of the initial and final particle spin-tensors and with effective propagators for the intermediate state particles. The magnitudes of these amplitudes are fit to the data.

All isobar channels combined account for over 70% of the charged double pion production cross section in the nucleon resonance excitation region. The remaining part of cross sections stems from direct 2π production processes, which are needed to describe backward strength in the π^- angular distributions and constrained by the π^+ and proton angular distributions (see Fig. 14). The strengths of the direct 2π production mechanisms, shown in bottom row of Fig. 13, have been fitted to the CLAS cross section data [142, 143, 144, 145] and can be found in [178].

Within the framework of the JM approach we achieved a good description of the 2π data over the entire kinematic range covered by the measurements. As a typical example, the model description of the nine 1-fold differential cross sections at $W = 1.51$ GeV and $Q^2 = 0.425$ GeV^2 are presented in Fig. 14 together with the contributing mechanisms. The different mechanism result in qualitatively different shapes of their respective contributions to various observables. The successful simultaneous description of the nine 1-fold differential cross sections enables us to identify the essential contributing processes and to access their dynamics at the phenomenological level. The extension of this approach to higher masses and higher Q^2 using data obtained at 6 GeV beam energy is currently underway. It will also provide new information on the mechanism that may be relevant for the phenomenological analysis of 2π data at the 12 GeV upgrade.

The amplitudes of non-resonant mechanisms derived from fitting the JM parameters to these data may also be used as input for N^* studies based on the global multi-channel analysis in a fully coupled-channel approach that is currently being developed at EBAC [186, 187, 188].

The separation of resonant and non-resonant contributions based on the JM model parameters are shown in Fig. 15. Resonant and non-resonant parts have qualitatively different shapes in all observables. This allows us to isolate the resonant contributions and to extract

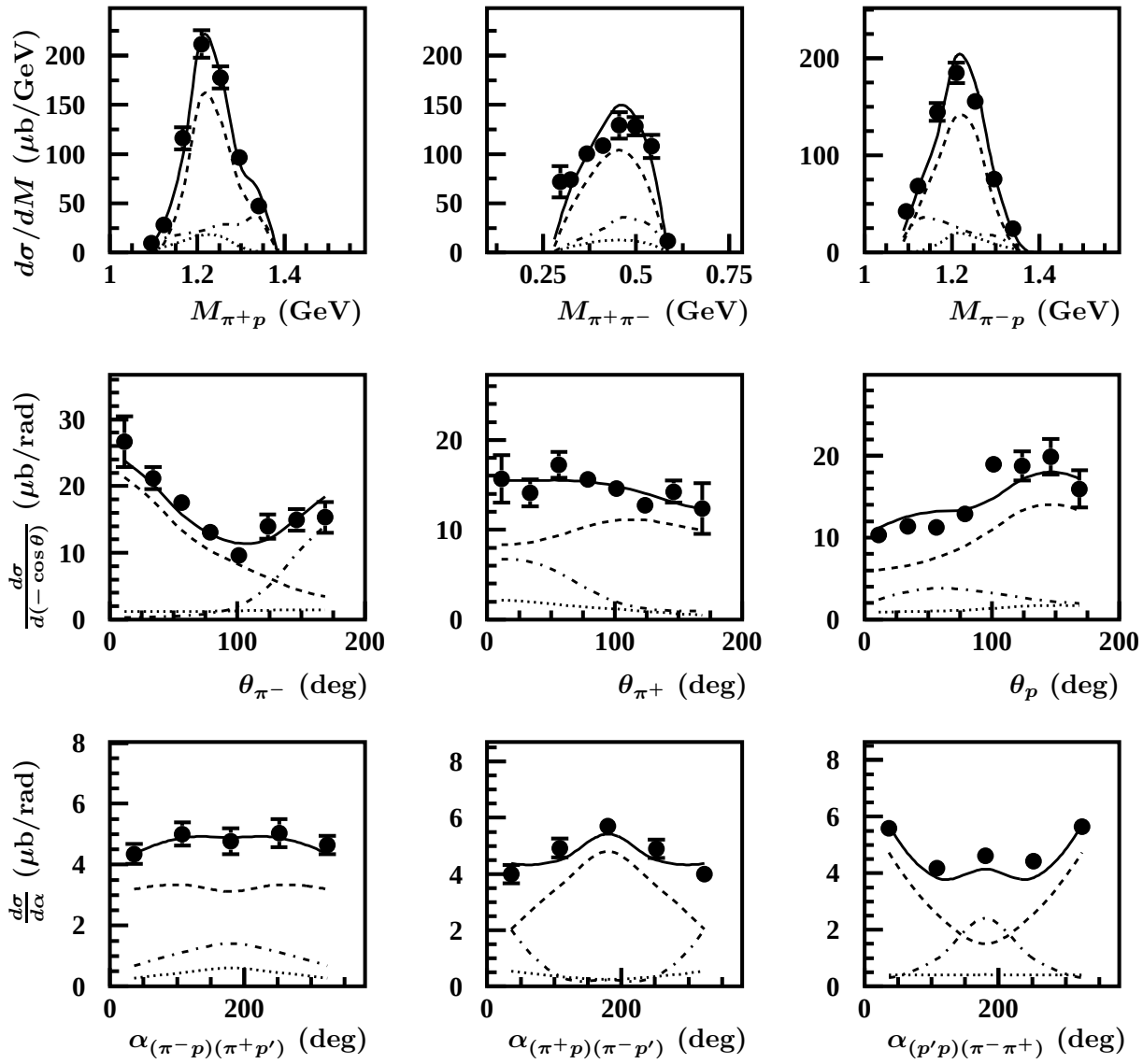

FIG. 14: Description of the CLAS charged double pion differential cross sections at $W = 1.51$ GeV and $Q^2 = 0.425\ GeV^2$ within the framework of the JM model. Full calculations are shown by the solid lines. Contributions from $\pi^-\Delta^{++}$ and $\pi^+\Delta^0$ isobar channels are shown by the dashed and dotted lines, respectively, and contributions from the direct charged double pion production processes are shown by the dot-dashed lines.

the N^* electrocoupling parameters.

N* electrocoupling parameters from single and double meson electroproduction

The CLAS data have enabled us for the first time to determine the $P_{11}(1440)$, $D_{13}(1520)$ and $S_{11}(1535)$ electrocoupling parameters over a wide range of photon virtualities by analyzing the two major exclusive channels: 1π and 2π electroproduction. These analyses

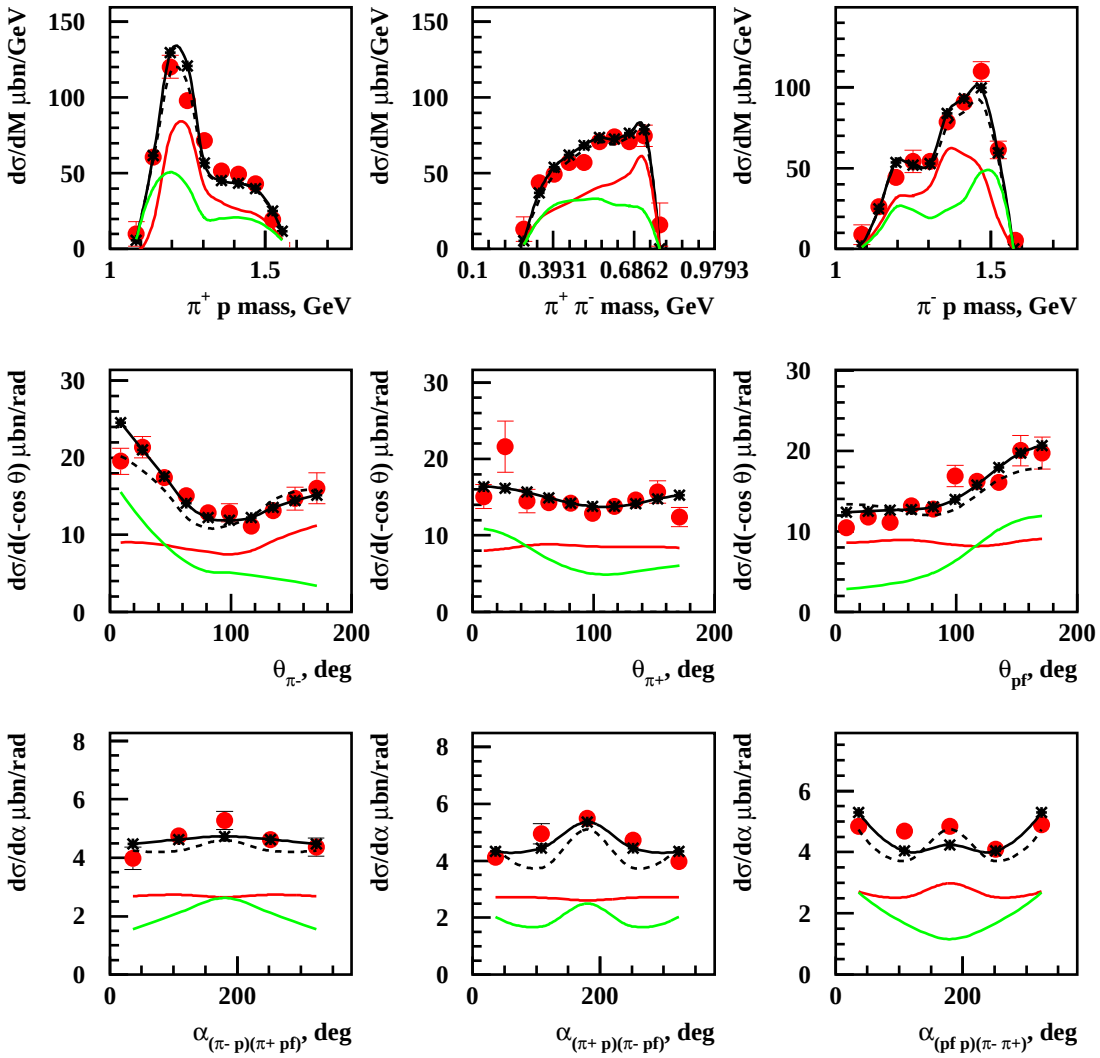

FIG. 15: Resonant (red lines) and non-resonant (green lines) contributions to the charged double pion differential cross sections at $W = 1.71$ GeV and $Q^2 = 0.65$ GeV^2. The full JM calculation is shown by black lines, whereas the solid and dashed lines correspond to two different sets of $A_{1/2}$, $A_{3/2}$ electrocoupling amplitudes for $3/2^+(1720)$ candidate state.

have been carried out within the framework of the approaches described above. The electrocoupling parameters of the $P_{11}(1440)$ and $D_{13}(1520)$ states are shown in Fig. 16. The agreement of the results obtained from the analyses of 1π and 2π channels is highly significant since the 1π and 2π meson electroproduction channels have completely different non-resonant amplitudes. The successful description of the large body of data on 1π and

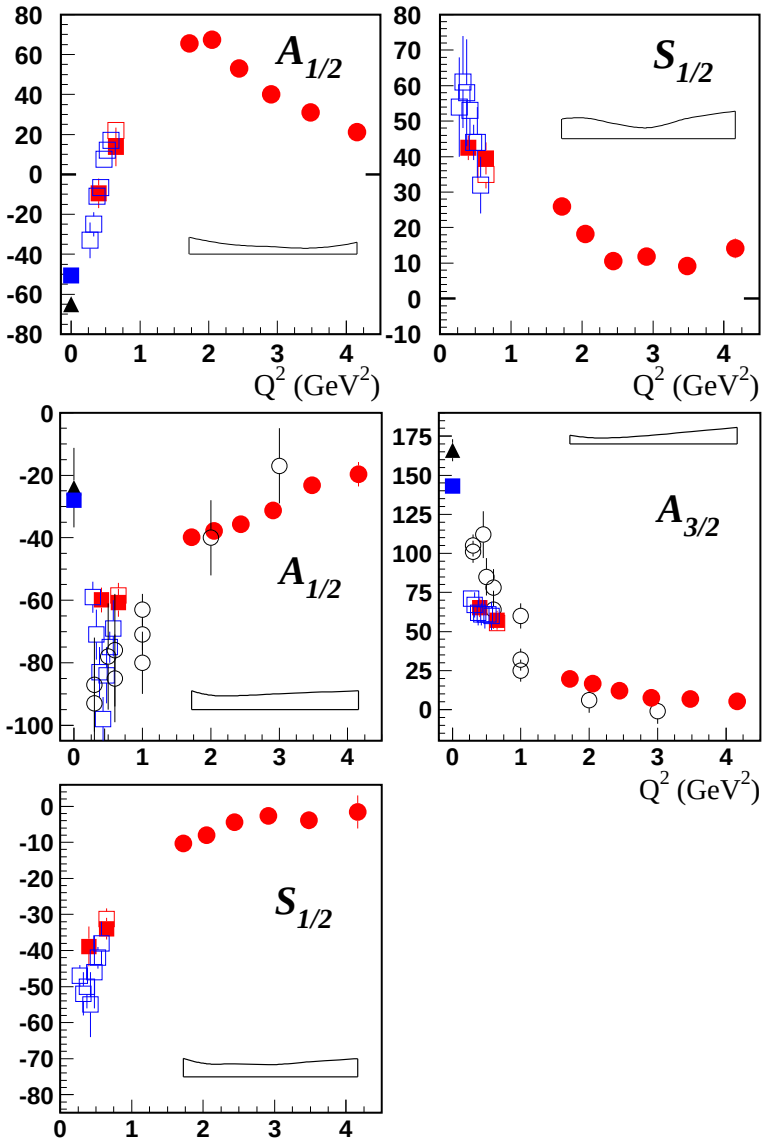

FIG. 16: Electrocoupling parameters of the $P_{11}(1440)$ (top row) and $D_{13}(1520)$ (middle and bottom rows) on the proton in units of 10^{-3} GeV$^{-1/2}$. CLAS results [171, 172, 173, 191] of the 1π production data are represented by the red circles and squares. Open squares are for the combined analysis of the 1π and 2π channel [172]. Blue open squares are the results of the 2π data [176, 177] at low Q^2. World data from $1\pi^\circ$ electroproduction, available before CLAS, are represented by black open circles.

2π electroproduction with almost the same values for the $P_{11}(1440)$ and $D_{13}(1520)$ electrocoupling parameters, shows the capability of the analyses methods to provide a reasonable evaluation of the resonance parameters.

The resonant part increases relative to the non-resonant part with W and Q^2. At $W > 1.65$ GeV and $Q^2 > 0.5$ GeV^2 it becomes the largest contribution (see Fig. 15). The 2π electroproduction channel hence offers the best opportunity to study higher-lying

resonances ($W > 1.65$ GeV). The majority of these states decay dominantly by 2π emission. Therefore, the combined analysis of 1π and 2π electroproduction opens the realistic possibility of accessing the electrocoupling parameters of the majority of excited states on the proton.

The results obtained from the 1π and 2π data represent reasonable, initial estimates of the Q^2 evolution of the N^* electrocoupling parameters. This information will be checked and improved in a global and complete coupled-channel analysis of major meson electroproduction channels that incorporates the amplitudes of non-resonant electroproduction mechanisms extracted from the CLAS data using the phenomenological models described above. This program requires a joint effort between Hall B and EBAC at Jefferson Lab.

VIII. STATUS OF THE EXITED BARYONS ANALYSIS CENTER

EBAC Strategy

The objective of EBAC is more than just performing the partial-wave analysis of the world data of the πN, γN and $N(e, e')$ reactions. We not only want to extract the N^* parameters, but also want to map out the quark-gluon substructure of N^* states. Thus it requires a full dynamical coupled-channels analysis [186] which accounts for both the unitarity conditions and the reaction mechanisms at short distances. The channels included in the current analysis are two-particles $\gamma^* N, \pi N, \eta N, K\Lambda, K\Sigma, \omega N$ states and the crucial three-particle $\pi\pi N$ state which has $\pi\Delta, \rho N, \sigma N$ resonant components.

The resonance parameters are extracted [192] from the poles on the unphysical sheets of the complex-energy plane. Within the Hamiltonian formulation of the constructed coupled-channel model, this method is capable of distinguishing the resonances originating either from the meson-baryon attractive forces or from the excitations of the quark-gluon degrees of freedom of the nucleon. Clearly, this approach is essential for interpreting the extracted N^* parameters in terms of the predictions from hadron models and LQCD.

Status of EBAC Analysis

The analysis of $\pi N, \gamma^* N \to \pi N, \eta N, \pi\pi N$ has been performed [193, 194, 195, 196, 197]. The resonance parameters of the low-lying N^* states with masses below about 1.7 GeV (red

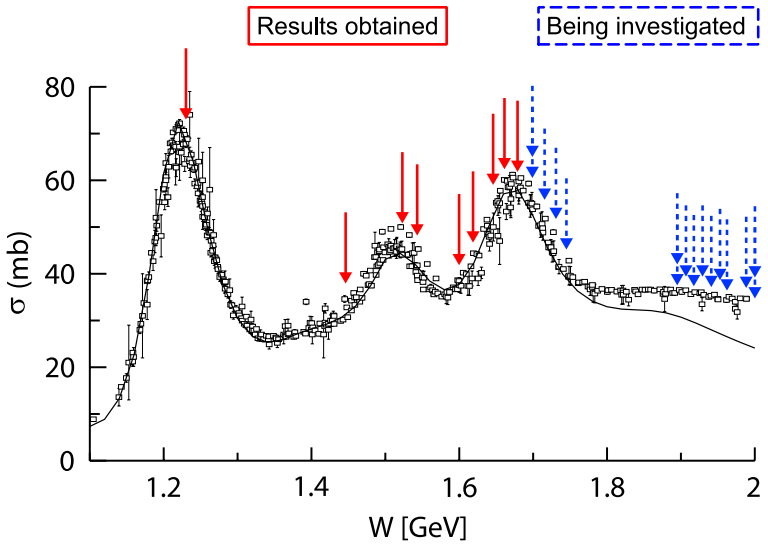

FIG. 17: The N^* positions listed by the Particle Data Group are identified with the $\pi^- p$ total cross sections. The solid curve is from EBAC's model [194].

arrows in Fig.17) have been extracted. In Fig.18, we show the comparison of the N-$\Delta(1232)$ transition form factors G_M, G_E, and G_C vs Q^2 extracted by EBAC from world data with the LQCD results from Ref. [198]. In Fig.19, we show that the discrepancies between the $\gamma N \to \Delta(1232), N^*(1440), N^*(1520)$ form factors predicted by the constituent quark models (dotted curves) and the empirical values from CLAS collaboration could be accounted for by including the meson-baryon dressing (meson cloud) effects (red dashed curves) predicted by the EBAC collaboration.

The higher mass N^* states (dashed arrows in Fig.17), suggested by Particle Data Group, are still being investigated. The main task is to include $K\Lambda$, $K\Sigma$, and ωN channels in the analysis. Furthermore an effort has been devoted to recover the old data of $\pi N \to \pi\pi N$ reactions which are essential in pinnig down the higher mass N^* states. New data from new hadron facilities, such as JPARC in Japan, perhaps will be essential in making conclusive determinations of these "elusive" N^* states.

The constructed coupled-channel model can be extended to include other resonant channels, such as the $\pi N^*(D_{13}, 1520), \pi N^*(F_{15}, 1680), \pi\Delta(P_{33}, 1600)$ channels suggested by the CLAS collaboration, if necessary. We are also investigating how the K-matrix models, used in the data analysis by the CLAS collaboration (described in section VII), the Mainz group, and the Bonn group, can be related to EBAC's dynamical approach. This will then further strengthen the theory-experiment joint effort in extracting the parameters of the higher mass

N^*'s indicated in Fig.17.

With the data from 12 GeV upgrade, the EBAC analysis needs to be extended to account for reaction mechanisms at high momentum transfer. It is necessary to describe the nonresonant mechanisms directly in terms of quark-gluon degrees of freedom. The results from DSE models, described in section III, will be used to make progress in this direction.

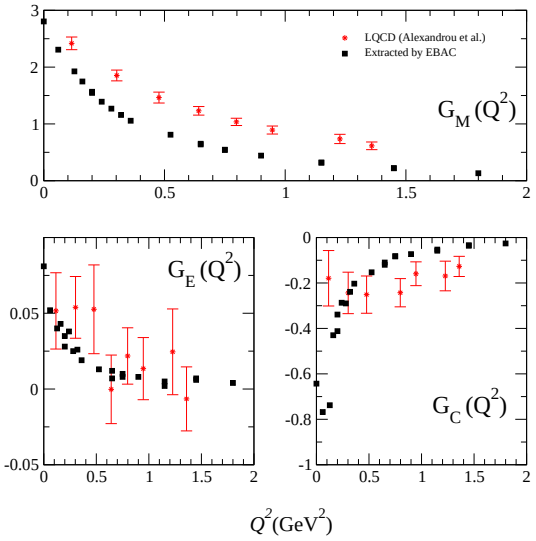

FIG. 18: The N-$\Delta(1232)$ transition form factors G_M, G_E, and G_C vs Q^2. Empirical values (solid squares) are extracted by EBAC from world data within a dynamical model. The LQCD results are from Ref. [198].

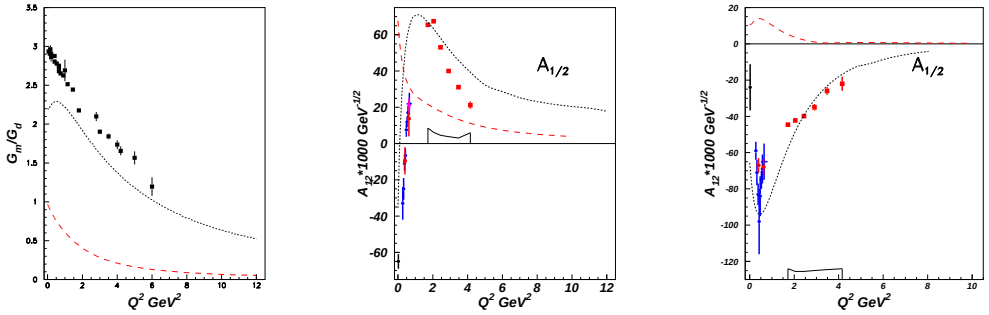

FIG. 19: The N-N^* transition form factors and helicity amplitudes. Left panel: Magnetic form factor for the N-$\Delta(1232)$ transition normalized to the dipole form factor. Center panel: Transition helicity amplitude $A_{1/2}$ for N-$N^*(1440)$. Right panel: Transition helicity amplitude $A_{1/2}$ for N-$N^*(1520)$. The results from CLAS/world experimental data analyses are shown by the data points [147, 148, 177, 190, 191]. The red and blue symbols are the results from analyses of 1π and 2π exclusive channels, respectively. The curves are from Constituent Quark Model calculations (dotted), described in section VI, and from meson-baryon dressing contributions predicted by the EBAC (dashed).

Acknowledgement

The authors are thankful to Dr. L. Elouadrhiri for useful discussions and important support. We express our gratitude to the Staff Services group at Jefferson Lab, especially to Mrs. S. Schatzel, the Electromagnetic N–N^* Transition Form Factors Workshop Secretary, for her invaluable administrative support of this very successful scientific meeting.

[1] L.A. Copley, G. Karl, E. Obryk, Nucl. Phys.**B13**, 303 (1969).

[2] N. Isgur and G. Karl, Phys. Rev. **D19**, 2653 (1979); S. Capstick and N. Isgur, Phys. Rev. D 34, 2809 (1986).

[3] G. Morpurgo, Physics **2**, 95 (1965).

[4] I. C. Cloet, D. B. Leinweber and A. W. Thomas, Phys. Rev. C **65**, 062201 (2002) [arXiv:hep-ph/0203023].

[5] I. G. Aznauryan, Phys. Lett. B **316**, 391 (1993).

[6] S. Capstick, B. Keister, Phys. Rev. **D51**,3598 (1995).

[7] B. Julia-Diaz, D. O. Riska, and F. Coester, Phys. Rev. **C 69**, 035212 (2004).

[8] I. G. Aznauryan, Phys. Rev. **C76**, 025212 (2007).

[9] M. Aiello, M. M. Giannini, E. Santopinto, J. Phys. G: Nucl. Part. Phys. **24**, 753 (1998).

[10] E.De Sanctis, M.M. Giannini, E. Santopinto, A. Vassallo, Phys. Rev. **C76**, 062201 (2007).

[11] C.S. An, Q.B. Li, D.O. Riska, B.S. Zou, Phys.Rev. **C74**, 055205 (2006), Erratum-ibid. **C75**, 069901 (2007).

[12] B.S. Zou, D.O. Riska, Phys.Rev. Lett. **95**, 072001 (2005).

[13] Q.B. Li, D.O. Riska, Nucl.Phys. **A766**, 172 (2006).

[14] C. D. Roberts, arXiv:0712.0633 [nucl-th] Prog. Part. Nucl. Phys. **61**, 50 (2008), arXiv:0712.0633 [nucl-th].

[15] V.Pascalutsa, M Vanderhaeghen and S. N Yang , Physics Reports **437**,125 (2007).

[16] M. V. Polyakov and K.M.Semenov-Tian-Shansky, arXiv:0811.2901 [hep-ph].

[17] http://conferences.jlab.org/EmNN/

[18] H. W. Lin *et al.*, Phys. Rev. D **79**, 034502 (2009), arXiv:0810.3588 [hep-lat].

[19] S. Basak *et al.*, Phys. Rev. D **72**, 094506 (2005) [arXiv:hep-lat/0506029].

[20] J. M. Bulava *et al.*, Phys. Rev. D **79**, 034505 (2009) arXiv:0901.0027 [hep-lat].

[21] J. J. Dudek, R. G. Edwards, N. Mathur and D. G. Richards, Phys. Rev. D **77**, 034501 (2008) [arXiv:0707.4162 [hep-lat]].

[22] H. W. Lin, S. D. Cohen, R. G. Edwards and D. G. Richards, arXiv:0803.3020 [hep-lat].

[23] H. W. Lin, S. D. Cohen, R. G. Edwards, K. Orginos and D. G. Richards, arXiv:0810.5141 [hep-lat].

[24] G. Krein, C. D. Roberts and A. G. Williams, Int. J. Mod. Phys. A **7** (1992) 5607

[25] J. Glimm and A. Jaffee, *Quantum Physics. A Functional Point of View* (Springer-Verlag, New York, 1981)

[26] A. Deur, V. Burkert, J. P. Chen and W. Korsch, Phys. Lett. B **650** (2007) 244.

[27] P. Maris, C. D. Roberts and P. C. Tandy, Phys. Lett. B **420** (1998) 267.

[28] M. S. Bhagwat, M. A. Pichowsky, C. D. Roberts and P. C. Tandy, *Phys. Rev.* C **68** (2003) 015203;

[29] M. S. Bhagwat and P. C. Tandy, AIP Conf. Proc. **842** (2006) 225.

[30] P. O. Bowman, *et al.*, *Phys. Rev.* D **71** (2005) 054507.

[31] C. D. Roberts and A. G. Williams, Prog. Part. Nucl. Phys. **33** (1994) 477.

[32] M. S. Bhagwat, I. C. Cloët and C. D. Roberts, "Covariance, Dynamics and Symmetries, and Hadron Form Factors," arXiv:0710.2059 [nucl-th].

[33] M. Gopfert and G. Mack, Commun. Math. Phys. **82** (1981) 545.

[34] A. Bashir, A. Raya, I. C. Cloet and C. D. Roberts, Phys. Rev. C **78** (2008) 055201.

[35] C. D. Roberts and S. M. Schmidt, Prog. Part. Nucl. Phys. **45** (2000) S1.

[36] R. Alkofer and L. von Smekal, Phys. Rept. **353** (2001) 281.

[37] P. Maris and C. D. Roberts, Int. J. Mod. Phys. E **12** (2003) 297.

[38] C. D. Roberts, M. S. Bhagwat, A. Höll and S. V. Wright, Eur. Phys. J. ST **140** (2007) 53.

[39] H. J. Munczek, Phys. Rev. D **52** (1995) 4736.

[40] A. Bender, C. D. Roberts and L. Von Smekal, Phys. Lett. B **380** (1996) 7.

[41] A. Bender, W. Detmold, C. D. Roberts and A. W. Thomas, Phys. Rev. C **65** (2002) 065203.

[42] M. S. Bhagwat, *et al.*, Phys. Rev. C **70** (2004) 035205.

[43] P. Maris and C. D. Roberts, Phys. Rev. C **56** (1997) 3369.

[44] A. Höll, A. Krassnigg and C. D. Roberts, *Phys. Rev.* C 70 (2004) 042203(R)

[45] A. Höll, *et al.*, *Phys. Rev.* C 71 (2005) 065204

[46] C. McNeile and C. Michael [UKQCD Collaboration], Phys. Lett. B **642** (2006) 244.

[47] M. A. Ivanov, Yu. L. Kalinovsky, P. Maris and C. D. Roberts, Phys. Lett. B **416** (1998) 29.

[48] M. A. Ivanov, Yu. L. Kalinovsky and C. D. Roberts, Phys. Rev. D 60 (1999) 034018.

[49] M. S. Bhagwat, A. Krassnigg, P. Maris and C. D. Roberts, Eur. Phys. J. A **31** (2007) 630.

[50] P. Maris and P. C. Tandy, Phys. Rev. C **60** (1999) 055214.

[51] P. Maris and P. C. Tandy, Phys. Rev. C 62 (2000) 055204; Nucl. Phys. Proc. Suppl. **161**

(2006) 136.

[52] M. A. Ivanov, J. G. Korner, S. G. Kovalenko and C. D. Roberts, Phys. Rev. D **76** (2007) 034018.

[53] R. Alkofer, A. Höll, M. Kloker, A. Krassnigg and C. D. Roberts, Few Body Syst. **37** (2005) 1.

[54] A. Holl, R. Alkofer, M. Kloker, A. Krassnigg, C. D. Roberts and S. V. Wright, Nucl. Phys. A **755** (2005) 298.

[55] V. V. Flambaum, A. Holl, P. Jaikumar, C. D. Roberts and S. V. Wright, Few Body Syst. **38** (2006) 31.

[56] I. C. Cloët, G. Eichmann, V. V. Flambaum, C. D. Roberts, M. S. Bhagwat and A. Höll, Few Body Syst. **42** (2008) 91.

[57] R. T. Cahill, C. D. Roberts and J. Praschifka, Austral. J. Phys. **42** (1989) 129.

[58] R. T. Cahill, C. D. Roberts and J. Praschifka, Phys. Rev. D **36** (1987) 2804.

[59] G. Eichmann, R. Alkofer, I. C. Cloët, A. Krassnigg and C. D. Roberts, Phys. Rev. C **77** (2008) 042202(R).

[60] G. Eichmann, I. C. Cloët, R. Alkofer, A. Krassnigg and C. D. Roberts, "On unifying the description of meson and baryon properties," arXiv:0810.1222 [nucl-th].

[61] A. Ali Khan, *et al.*, Phys. Rev. D **65** (2002) 054505.

[62] C. R. Allton, W. Armour, D. B. Leinweber, A. W. Thomas and R. D. Young, Phys. Lett. B **628** (2005) 125.

[63] A. Ali Khan, *et al.*, [QCDSF-UKQCD Collaboration], Nucl. Phys. B **689** (2004) 175.

[64] R. Frigori, C. Gattringer, C. B. Lang, M. Limmer, T. Maurer, D. Mohler and A. Schafer, PoS **LAT2007** (2007) 114.

[65] D. B. Leinweber, A. W. Thomas and R. D. Young, Phys. Rev. Lett. **92** (2004) 242002.

[66] I. C. Cloët, G. Eichmann, B. El-Bennich, T. Klähn and C. D. Roberts, Few Body Syst. **46** 1 (2009).

[67] O. Gayou, *et al.* [JLab Hall A Collaboration], Phys. Rev. Lett. **88** (2002) 092301.

[68] V. Punjabi *et al.*, Phys. Rev. C **71** (2005) 055202 [Erratum-ibid. C **71** (2005) 069902]

[69] I. A. Qattan *et al.*, Phys. Rev. Lett. **94** (2005) 142301.

[70] R. C. Walker *et al.*, Phys. Rev. D **49** (1994) 5671 .

[71] J. J. Kelly, Phys. Rev. C **70** (2004) 068202.

[72] R. Madey *et al.* [E93-038 Collaboration], Phys. Rev. Lett. **91** (2003) 122002.

[73] C. D. Roberts, Nucl. Phys. A **605** (1996) 475.

[74] P. Maris and C. D. Roberts, Phys. Rev. C **58** (1998) 3659.

[75] I. C. Cloet, W. Bentz and A. W. Thomas, Phys. Rev. Lett. **95** (2005) 052302.

[76] I. C. Cloet, W. Bentz and A. W. Thomas, Phys. Lett. B **621** (2005) 246.

[77] I. C. Cloet, W. Bentz and A. W. Thomas, Phys. Lett. B **642** (2006) 210.

[78] I. C. Cloet, W. Bentz and A. W. Thomas, Phys. Lett. B **659** (2008) 214.

[79] I. C. Cloet, W. Bentz and A. W. Thomas, "N $\to \Delta$ transition in a covariant quark-diquark model," in progress.

[80] V. V. Frolov *et al.*, Phys. Rev. Lett. **82** (1999) 45.

[81] M. Ungaro *et al.* [CLAS Collaboration], Phys. Rev. Lett. **97** (2006) 112003.

[82] D. Nicmorus, University of Graz, private communication.

[83] V. M. Braun, A. Lenz, N. Mahnke and E. Stein, Phys. Rev. D **65**, 074011 (2002).

[84] V. M. Braun, A. Lenz and M. Wittmann, Phys. Rev. D **73**, 094019 (2006).

[85] P. Stoler. Contribution to these proceedings.

[86] C. E. Carlson, Phys. Rev. D **34**, 2704 (1986).

[87] C. E. Carlson and J. L. Poor, Phys. Rev. D **38**, 2758 (1988).

[88] V. M. Braun *et al.*, Phys. Rev. D **74**, 074501 (2006).

[89] T. Kaltenbrunner, M. Göckeler and A. Schäfer, Eur. Phys. J. C **55**, 387 (2008).

[90] M. Göckeler *et al.*, Nucl. Phys. B **812**, 205 (2009), arXiv:0810.3762 [hep-lat].

[91] V. M. Braun *et al.*, arXiv:0811.2712 [hep-lat].

[92] N. Warkentin *et al.*, "Wave functions of the nucleon and its parity partner from lattice QCD," arXiv:0811.2212 [hep-lat].

[93] V. M. Braun, A. Lenz, G. Peters and A.V. Radyushkin, Phys. Rev. D **73** (2006) 034020.

[94] V. M. Braun, D. Y. Ivanov, A. Lenz and A. Peters, Phys. Rev. D **75**, 014021 (2007).

[95] V. M. Braun, D. Y. Ivanov and A. Peters, Phys. Rev. D **77**, 034016 (2008).

[96] V. M. Braun *et al.*, arXiv:0902.3087 [hep-ph].

[97] M. Dalton et al., hep-ex ,arXiv:0804.3509v3

[98] K. Passek-Kumericki and G. Peters, Phys. Rev. D **78**, 033009 (2008).

[99] V. Braun. Contribution to the these proceedings.

[100] M. Diehl, T. Feldmann, R. Jakob and P. Kroll, Eur. Phys. J. C **39**, 1 (2005), [arXiv:hep-

ph/0408173].

[101] L.L. Frankfurt, M.V. Polyakov, M. Strikman, M. Vanderhaeghen, Phys. Rev. Lett. **84** 2589,(2000).

[102] K. Goeke, M.V. Polyakov, M. Vanderhaeghen, Prog. Part. Nucl. Phys. **47**, 401 (2001) .

[103] Jones H.F., M.D. Scadron, Ann. of Phys. **81**, 1 (1973).

[104] P. Stoler, Phys.Rev.Lett., **91**,172303 (2003).

[105] V.Pascalutsa, M Vanderhaeghen and S. N Yang , Physics Reports **437**,125 (2007)

[106] M. Burkardt, Phys.Rev.**D62**:071503(2000), Erratum-ibid.D66:119903(2002).

[107] I. I. Balitsky, V. M. Braun and A. V. Kolesnichenko, Nucl. Phys. B **312**, 509 (1989); V. L. Chernyak and I. R. Zhitnitsky,Nucl. Phys. B **345**, 137 (1990).

[108] V. M. Braun, talk at the EMNN* Workshop, JLAB, October 2008; also presented at PANIC2008 poster session, Eilat, November 2008.

[109] N. Isgur and G. Karl, *Phys. Rev.* **D18**, 4187 (1978); Phys. Rev. **D 19**, 2653 (1979).

[110] S. Capstick and N. Isgur, Phys. Rev. **D 34**,2809 (1986).

[111] F. Cardarelli, E. Pace, G. Salme and S. Simula, Phys. Lett. B **357**, 267 (1995).

[112] R. Bijker, F. Iachello and A. Leviatan, Ann. Phys. (N.Y.) **236**, 69 (1994).

[113] M. Ferraris, M.M. Giannini, M. Pizzo, E. Santopinto and L. Tiator, Phys. Lett. **B364**, 231 (1995).

[114] L. Ya. Glozman and D.O. Riska, Phys. Rep. **C268**, 263 (1996); L. Ya. Glozman, W. Plessas, K. Varga, R.F. Wagenbrunn, Phys. Rev. **D 58**, 094030 (1998)

[115] U. Loring, K. Kretzschmar, B. Ch. Metsch, H. R. Petry, Eur. Phys. **J. A10**, 309 (2001); U. Loring, B.Ch. Metsch, H. R. Petry, Eur. Phys. **J. A10**, 395 (2001); U. Loring, B.Ch. Metsch, and H. R. Petry, Eur. Phys. **J. A10**, 447 (2001).

[116] M. De Sanctis, E. Santopinto, M.M. Giannini, Eur. Phys. J. **A2**, 403 (1998).

[117] E. Pace, G. Salmé, F. Cardarelli and S. Simula, Nucl. Phys. **A666**, 33 (2000).

[118] S. Boffi, L. Y. Glozman, W. Klink, W. Plessas, M. Radici and R. F. Wagenbrunn, Eur. Phys. J. **A14**, 17 (2002).

[119] T. Melde, et al. Phys. Rev. **D 76**, 074020 (2007).

[120] M.De Sanctis, M.M. Giannini, E. Santopinto, A. Vassallo, Phys. Rev. **C76**, 062201 (2007).

[121] S. Capstick et al., Eur. Phys. J. **A35**, 253 (2008).

[122] P. Geiger and N. Isgur, Phys. Rev. Lett. **67**, 1066 (1991); Phys. Rev. **D 44**, 799 (1991);

Phys. Rev. **D 47**, 5050 (1993); P. Geiger and N. Isgur, Phys. Rev. **D 55**, 299 (1997).

[123] R. Bijker and E. Santopinto, arXiv:0812.0614 [nucl-th]; arXiv:0809.4424; NSTAR2007: arXiv:0809.2299 and arXiv:0809.2296; MENU2007: arXiv:0806.3028; AIP Conf. Proc. **947**, 168 (2007).

[124] L. Tiator, D. Drechsel, S. Kamalov, M.M. Giannini, E. Santopinto, A. Vassallo, Eur. Phys. J. **A 19** (Suppl.1), 55 (2004).

[125] S. Kamalov, S.N. Yang, D. Drechsel, O. Hanstein, L. Tiator, Phys. Rev. **C 64** (2001) 032201.

[126] C. S. An, B. Zou, Eur. Phys. J.**A39**, 195 (2009); B.Julia-Diaz, D.O.Riska, Nucl. Phys. **A780**, 175 (2006).

[127] R. Petronzio, S. Simula, G. Ricco, Phys. Rev. **D 67**, (2003) 094004.

[128] Q. Zhao, F. E. Close, Phys. Rev. Lett. **91**, (2003) 022004.

[129] K. Joo et al., Phys. Rev. Lett. **88**, 122001 (2002).

[130] K. Joo et al., Phys. Rev. **C68**, 032201 (2003).

[131] K. Joo et al., Phys. Rev. **C70**, 042201 (2004).

[132] K. Joo et al., Phys. Rev. **C72**, 058202 (2005).

[133] H. Egiyan et al, Phys. Rev, **C73**, 025204 (2006).

[134] A. Biselli et al., Phys. Rev. **C68**, 035202 (2003).

[135] A. S. Biselli *et al.*, Phys. Rev. C **78**, 045204 (2008)

[136] K. Park et al., Phys. Rev. **C77**, 015208 (2008).

[137] R. Thompson et al., Phys. Rev. Lett. **86**, 1702 (2001).

[138] H. Denizli et al., Phys. Rev. **C76**, 015204 (2007).

[139] P. Ambrozewicz et al., Phys. Rev. **C75**, 045203 (2007).

[140] D. Carman et al., Phys. Rev. Lett. **90**, 131804 (2003).

[141] R. De Vita et al., Phys. Rev. Lett. **88**, 082001 (2002).

[142] M. Ripani et al., Phys. Rev. Lett. **91**, 022002 (2003).

[143] G. V. Fedotov et al., Bull. of Russian Acad. of Scince **71**, 328 (2007).

[144] G. V. Fedotov et al., Phys. of Atom. Nucl, 1309 (2008).

[145] G. V. Fedotov et al.,Phys. Rev. **C79**, 015204 (2009), arXiv:0809.1562[nucl-ex].

[146] V. D. Burkert and T.S.-H. Lee, in "Electromagnetic Interactions and Hadronic Structure", ed by F. Close, S. Donnachie, G. Shaw, Cambridge Monographs on Particle Physics, Nuclear Physics and Cosmology 77 (2007).

[147] V. D. Burkert, Prog. Part Nucl. Phys. **55**, 108 (2005).

[148] V. Burkert and T. S.-H. Lee, Int. J. Mod. Phys. **E13**, 1035 (2004).

[149] R. L. Walker, Phys. Rev. **182**, 1729 (1969).

[150] G. F. Chew, M. L. Goldberger, F. E. Low, and Y. Nambu, Phys. Rev. **106**, 1345 (1957).

[151] S. Fubini, Y. Nambu, and V. Watagin, Phys. Rev. **111**, 329 (1958).

[152] D. Drechsel, O. Hanstein, S. Kamalov, and L. Tiator, Nucl. Phys. A **645**, 145 (1999).

[153] L. Andivanis et al., Phys. Rev. D **4**, 45 (1971).

[154] Ch. Berger et al., Phys. Lett. B **35**, 87 (1971).

[155] W. Bartel et al., Nucl. Phys. B **58**, 429 (1973).

[156] A. F. Still et al., Phys. Rev. D **48**, 29 (1993).

[157] R. C. Walker et al., Phys. Rev. D **49**, 5671 (1994).

[158] L. Andivanis et al., Phys. Rev. D **50**, 5491 (1994).

[159] M. K. Jones et al., Phys. Rev. Lett. **84**, 1398 (2000).

[160] O. Gayou et al., Phys. Rev. C **64**, 038202 (2001).

[161] A. Lung et al., Phys. Rev. Lett. **70**, 718 (1993).

[162] W. K. Brooks et al., Nucl. Phys. A **755**, 261 (2005).

[163] J. Arrington, W. Melnitchouk, J. A. Tjon, Phys. Rev. C **76**, 035205 (2007).

[164] C. J. Bebek et al., Phys. Rev. **D13**, 25 (1976).

[165] C. J. Bebek et al., Phys. Rev. **D17**, 1693 (1978).

[166] T. Horn et al., Phys. Rev. Lett. **97**, 192001 (2006).

[167] V. Tadevosyan et al., Phys. Rev. C **75**, 055205 (2007).

[168] V. Eletski and Ya. Kogan, Yad. Fiz. **39**, 138 (1984).

[169] I. Aznauryan and K. Oganessyan, Phys. Lett. B **249**, 309 (1990).

[170] I. G. Aznauryan, Phys. Rev. C **67**, 015209 (2003).

[171] I. G. Aznauryan, V. D. Burkert, H. Egiyan, et al., Phys. Rev. C **71**, 015201 (2005).

[172] I. G. Aznauryan, V. D. Burkert, et al., Phys. Rev. C **72**, 045201 (2005).

[173] I. G. Aznauryan, V. D. Burkert, et al., Phys. Rev. C **78**, 045209 (2008).

[174] V. I. Mokeev and V. D. Burkert, J. Phys. Conf. Ser **69**, 012019 (2007),hep-ph/0701056.

[175] V. I. Mokeev, V. D. Burkert, et al., Proc. of the Workshop on the Physics of Excited Nucleon. NSTAR2005, ed. by S.Capstick, V.Crede, P.Eugenio,hep-ph/0512164.

[176] V. I. Mokeev et al., arXiv: 0906.4081[hep-ph].

[177] V. I. Mokeev et al., Proceedings of the 11th Workshop on the Physics of Excited Nucleons. NSTAR2007, Springer, ed. by H-W. Hammer, V.Kleber, U.Thoma, H. Schmieden, arXiv:0710.5616[hep-ex]

[178] V. I. Mokeev et al., arXiv: 0809.4158[hep-ph].

[179] D. Luke and P. Söding Springer Tracts in Modern Physics 59, (1971).

[180] M. Ripani et al., Nucl. Phys. **A672**, 220 (2000).

[181] V. Mokeev et al., Phys. Atom. Nucl. **64**, 1292 (2001).

[182] V. Mokeev et al., Phys. Atom. Nucl. **66**, 1322 (2003).

[183] V. D. Burkert, et al., Phys. Atom. Nucl. **70**, 427 (2007).

[184] T. P. Vrana, S. A. Dytman and T-S. H. Lee, Phys. Rep. **32B**, 184 (2000).

[185] G. Penner and U. Mosel, Phys. Rev. **C65**, 055202 (2002).

[186] A. Matsuyama, T. Sato and T.-S. H. Lee, Phys. Rep. **439**, 193 (2007).

[187] T. S.-H. Lee, J. Phys. Conf. Ser. **69**, 012013 (2007).

[188] T. S.-H. Lee and L. C. Smith, J. Phys. **G34**, S83 (2007).

[189] I. G. Aznauryan, V. D. Burkert, et al., Phys. Rev. C **76**, 025212 (2009).

[190] I. G. Aznauryan *et al.*, CLAS Collaboration, Phys. Rev. C **78**, 045209 (2008).

[191] V. D. Burkert, AIP Conf. Proc. **1056**, 348 (2008).

[192] N. Suzuki, T. Sato, T.-S. H. Lee, Phys. Rev. C **79**, 025205 (2009), arXiv:0806.2043 [nucl-th].

[193] B. Julia-Diaz, T.-S. H. Lee, T. Sato, L.C. Smith, Phys. Rev. C **75**, 015205 (2007)

[194] B. Julia-Diaz, T.-S.H. Lee, A. Matsuyama, T. Sato, Phys.Rev. C **76**, 5201 (2007)

[195] B. Julia-Diaz, T.-S.H. Lee, A. Matsuyama, T. Sato, L.C. Smith ,Phys.Rev.C **77**, 045205 (2008).

[196] J. Durand, B. Julia-Diaz, T.-S.H. Lee, B. Saghai, T. Sato, Phys.Rev.C **78**, 025204 (2008).

[197] H. Kamano, B. Julia-Diaz, T.-S.H. Lee, A. Matsuyama, T. Sato, Phys. Rev. C **79**, 025206 (2009), arXiv:0807.2273 [nucl-th].

[198] Alexandrou P. deForcrand, T. Lippert, H. Neff, J. W. Negele, K. Schilling, W. Schroers, and A. Tsapalis, Phys. Rev. D 69, 114506 (2004); C. Alexandrou, P. de Forcrand, H. Neff, J. W. Negele, W. Schroers, and A. Tsapalis, Phys. Rev. Lett. 94, 021601 (2005); C. Alexandrou, T. Leontiou, J.W. Negele, and A. Tsapalis, hep-lat/0608025.